

1
2
3 | **Investigating ~~basin-scale~~ water budget dynamics in 18 river basins**
4 **across Tibetan Plateau through multiple datasets**

5 Wenbin Liu^a, Fubao Sun^{a,b*}, Yanzhong Li^a, Guoqing Zhang^{c,d}, Yan-Fang Sang^a,
6 Wee Ho Lim^{a,e}, Jiahong Liu^f, Hong Wang^a, Peng Bai^a

7
8 ^aKey Laboratory of Water Cycle and Related Land Surface Processes, Institute of Geographic
9 Sciences and Natural Resources Research, Chinese Academy of Sciences, Beijing 100101, China

10 ^bHexi University, Zhangye 734000, China ^cKey Laboratory of Tibetan Environmental Changes
11 and Land Surface Processes, Institute of Tibetan Plateau Research, Chinese Academy of Sciences,
12 Beijing 100101, China ^dCAS Center for Excellent in Tibetan Plateau Earth Sciences, Beijing
13 100101, China ^eEnvironmental Change Institute, Oxford University Centre for the Environment,
14 School of Geography and the Environment, University of Oxford, Oxford OX1 3QY, UK ^fKey
15 Laboratory of Simulation and Regulation of Water Cycle in River Basin, China Institute of Water
16 Resources and Hydropower Research, Beijing 100038, China

17
18 **Re-submitted to:** Hydrology and Earth System Sciences

19 **Corresponding Author:** Dr. Fubao Sun (Sunfb@igsnr.ac.cn), Key Laboratory of Water Cycle
20 and Related Land Surface Processes, Institute of Geographic Sciences and Natural Resources
21 Research, Chinese Academy of Sciences

22
23 | 2017/~~07~~10

Abstract The dynamics of basin-scale water budgets are not well understood nowadays over the Tibetan Plateau (TP) due to the lack of in situ hydro-climatic observations. In this study, we investigate the seasonal cycles and trends of water budget components (e.g., precipitation-P, evapotranspiration-ET and runoff-Q) in eighteen TP river basins during the period 1982-2011 through the use of multi-source datasets (e.g., in situ observations, satellite retrievals, reanalysis outputs and land surface model simulations). A water balance-based two-step procedure, which considers the changes in basin-scale water storage at the annual scale, is also adopted to calculate actual ET. The results indicated that precipitation (mainly snowfall from mid-autumn to next spring), which mainly concentrated during June-October (varied among different monsoons-impacted basins), was the major contributor to the runoff in TP basins. Increased P, ET and Q were found in most TP basins during the past 30 years except for the upper Yellow River basin and some sub-basins of Yalong River, which were mainly affected by the weakening East Asian Monsoon. Moreover, the aridity index (PET/P) and runoff coefficient (Q/P) decreased in most basins, which were in agreement with the warming and moistening climate in the Tibetan Plateau. The results obtained demonstrated the usefulness of integrating multi-source datasets to hydrological applications in the data-sparse regions. More generally, such approach might offer helpful insights towards understanding the water and energy budgets and sustainability of water resource management practices of data-sparse regions in a changing environment.

1 Introduction

As the highest plateau in the globe (the average elevation is higher than 4000 meters above the sea level), the Tibetan Plateau (TP, also called “the roof of the world” or “the third Pole”) is regarded as one of the most vulnerable regions under a warming climate and is exposed to strong interactions among atmosphere, hydrosphere, biosphere and cryosphere in the earth system (Duan and Wu, 2006; Yao et al., 2012; Liu et al., 2016b). It also serves as the “Asian water tower” from which some major Asian rivers such as Yellow River, Yangtze River, Brahmaputra River, Mekong River, Indus River, etc., originate, which is a vital water resource to support the livelihood of hundreds of millions of people in China and the neighboring Asian countries (Immerzeel et al., 2010; Zhang et al., 2013). Hence sound knowledge of water budget and hydrological regimes in TP river basins and ~~their~~ responses to the changing environment would have practical relevance for achieving sustainable water resource management and environmental protection in this part of the world (Yang et al., 2014; Chen et al., 2015).

Despite the importance of TP in this geographic region, advance in hydrological and land surfaces studies in this region has been limited by data scarcity (Zhang et al., 2007; Li F. et al., 2013; Liu X. et al., 2016). For instance, less than 80 observation stations (~10% of a total of ~750 observation station across China) have been established in TP by the Chinese Meteorological Administration (CMA) since the mid-20th century (Wang and Zeng, 2012). These stations are generally sparse and unevenly distributed at relatively low elevation regions (most stations are located in the eastern TP and few of them situated in the western parts), focus only on the meteorological variables and lack of other land surface observations such as

71 evapotranspiration, snow water equivalent and latent heat fluxes. In addition,
72 long-term observations of river discharge, ~~snow depth~~, lake depth and glacier melts in
73 the TP are also absent (Akhta et al., 2009; Ma et al., 2016). Therefore, the water
74 budget and hydrological regimes for each river basin of TP and their relation with
75 atmospheric circulations are poorly understood (Cuo et al., 2014; Xu et al., 2016).
76 Whilst this shortcoming could be resolved through installation of in-situ monitoring
77 systems (Yang et al., 2013; Zhou et al., 2013; Ma et al., 2015), the overall cost, labor
78 and technical support for ~~of~~ running the operational sites would be substantial.
79 Another workaround would be through modeling approach, i.e., feeding remote
80 sensing information and meteorological forcing data into physically-based land
81 surface model (LSM) to simulate the basin-wide water budget (Bookhagen and
82 Burbank, 2010; Xue et al., 2013; Zhang et al., 2013; Cuo et al., 2015; Zhou et al.,
83 2015; Wang et al., 2016). However, such approach is not immune from the issue of
84 data scarcity at multiple river basins (with varied sizes and/or terrain complexities) for
85 supporting model calibration and validation purposes (Li F. et al., 2014).
86
87 Most recently, several global (or regional) datasets relevant to the calculation of water
88 budget have been released. They include remote sensing-based retrievals (Tapley et al.,
89 2004; Zhang et al., 2010; Long et al., 2014; Zhang Y. et al., 2016), land surface model
90 (LSM) simulations (Rui, 2011), reanalysis outputs (Berrisford et al., 2011; Kobayashi
91 et al., 2015) and gridded forcing data interpolated from the in situ observations
92 (Harris et al., 2014). For example, there are many products related to terrestrial
93 evapotranspiration (ET) such as GLEAM_E (Global Land surface Evaporation: the
94 Amsterdam Methodology, Miralles et al., 2011a), MTE_E (a product integrated the
95 point-wise ET observation at FLUXNET sites with geospatial information extracted

from surface meteorological observations and remote sensing in a machine-learning algorithm, Jung et al., 2010), LSM-simulated ETs from Global Land Data Assimilation System version 2 (GLDAS-2) with different land surface schemes (Rodell et al., 2004), ETs from Japanese 55-year reanalysis (JRA55_E), the ERA-Interim global atmospheric reanalysis dataset (ERA-Interim) and the National Aeronautic and Space Administration (NASA) Modern Era Retrospective-analysis for Research and Application (MERRA) reanalysis data (Lucchesi, 2012). Moreover, there are also several global or regional LSM-based runoff simulations from GLDAS and the Variable Infiltration Capacity (VIC) model (Zhang et al., 2014). A few attempts have been made to validate multiple datasets for certain water budget components and to explore their possible hydrological implications. For example, Li X. et al. (2014) and Liu et al. (2016a) evaluated multiple ET estimates against the water balance method at annual and monthly time scales. Bai et al. (2016) assessed streamflow simulations of GLDAS LSMs in five major rivers over the TP based on the discharge observations. Although uncertainties might exist among different datasets with various spatial and temporal resolutions and calculated using different algorithms (Xia et al., 2012), they offer an opportunity to examine the general basin-wide water budgets and their uncertainties in gauge-sparse regions such as the TP considered in this study.

From the multiple datasets perspective, this study aims to investigate the water budget in 18 TP river basins distributed across the Tibetan Plateau; and evaluate seasonal cycles and annual trends of these water budget components. This paper is organized as follows: the datasets and methods applied in this study are described in Sect.2. The results of season cycles and annual trends of water budget components for the river

basins are presented and discussed in Sect.3. The uncertainties arise from employing multiple datasets are also discussed in the same section. In Sect.4, we generalize our findings which would be helpful for understanding the water balances of the river basins under constant influence of interplay between westerlies and monsoons (e.g., Indian monsoon, East Asian monsoon) in the Tibetan Plateau.

2 Data and methods

2.1 Multiple datasets used

2.1.1 Runoff, precipitation and terrestrial storage change

We obtained the observed daily runoff (Q) during the period 1982-2011 from the National Hydrology Almanac of China (Table 1). There are < 30% missing data in some gauging stations such as Yajiang, Tongren, Gandatan and Zelingou. Therefore, the VIC Retrospective Land Surface Dataset over China (1952–2012, VIC_IGSNRR simulated) with a spatial resolution of 0.25 degree and a daily temporal resolution from the Geographic Sciences and Natural Resources Research (IGSNRR), Chinese Academy of Sciences, is also used. This dataset is derived from the VIC model forced by the gridded daily observed meteorological forcing (IGSNRR_forcing) (Zhang et al., 2014). A degree-day scheme was used in the model to account for the influences of snow and glacier on hydrological processes.

In terms of precipitation (P), we used the gridded monthly precipitation dataset available at CMA (spatial resolution of 0.5 degree; 1961-2011; interpolated from observations of 2372 national meteorological stations using the Thin Plate Spline method) (Table 1). Since the reliability of this dataset might be restricted by the relatively sparse stations and complex terrain conditions of TP, we make an attempt to

incorporate two other precipitation datasets ((IGSNRR_forcing and Tropical Rainfall Measuring Mission TRMM 3B43 V7). The precipitation from IGSNRR forcing datasets (0.25 degree) was derived by interpolating gauged daily precipitation from 756 CMA stations based on the synergraphic mapping system algorithm (Shepard, 1984; Zhang et al., 2014) and was further bias-corrected using the CMA gridded precipitation.

<Table 1, here please, thanks>

To get the change in terrestrial storage (ΔS), we used three latest global terrestrial water storage anomaly and water storage change datasets (available on the GRACE Tellus website: <http://grace.jpl.nasa.gov/>) that were retrieved from the Gravity Recovery and Climate Experiment (GRACE, Tapley et al., 2004; Landerer and Swenson, 2012; Long et al., 2014). Briefly, they were processed separately at the Jet Propulsion Laboratory (JPL), the GeoForschungsZentrum (GFZ) and the Center for Space Research at the University of Texas (CSR). To minimize the errors and uncertainty of extracted ΔS , we averaged these GRACE retrievals (2002-2013) from different processing centers in this study.

2.1.2 Temperature, potential evaporation and ET

We obtained the monthly gridded temperature dataset (0.5 degree) from CMA; and potential evaporation (PET) dataset (0.5 degree, Harris et al., 2013) from Climatic Research Unit (CRU), University of East Anglia. Moreover, we used six global /regional ET products (four diagnostic products and two LSMs simulations, Table 21), namely (1) GLEAM_E (Miralles et al., 2010, 2011), which consists of three sources of ET (transpiration, soil evaporation and interception) for bare soil, short vegetation

and vegetation with a tall canopy calculated using a set of algorithm (www.gleam.eu),
 (2) GNoah_E simulated using GLDAS-2 with the Catchment Noah scheme
 (<http://disc.sci.gsfc.nasa.gov/hydrology/data-holdings>) (Rodell et al., 2004), (3)
 Zhang_E (Zhang et al., 2010), which is estimated using the modified
 Penman-Monteith equation forced with MODIS data, satellite-based vegetation
 parameters and meteorological observations (<http://www.nts.gov.au/project/et>), (4)
 MET_E (Jung et al., 2010) (<https://www.bgc-jena.mpg.de/geodb/projects/Home.php>),
 (5) VIC_E (Zhang et al., 2014) from VIC_IGSNRR simulations
 (http://hydro.igsnrr.ac.cn/public/vic_outputs.html) and (6) PML_E (Zhang Y. et al.,
 2016) computed from global observation-driven Penman-Monteith-Leuning (PML)
 model (<https://data.csiro.au/dap/landingpage?pid=csiro:17375&v=2&d=true>).

2.1.3 Vegetation and snow/glacier parameters

To quantify the dynamics of vegetation of each river basin, we applied the
 Normalized Difference Vegetation Index (NDVI) and the Leaf Area Index (LAI)
 (Table 1). Briefly, the NDVI data was obtained from the Global Inventory Modeling
 and Mapping Studies (GIMMS) (Turker et al., 2005)
 (https://nex.nasa.gov/nex/projects/1349/wiki/general_data_description_and_access/)
 while the LAI data was collected from the Global Land Surface Satellite (GLASS)
 products (<http://www.glcfc.umd.edu/data/lai/>) (Liang and Xiao, 2012). Whist the
 change in seasonal snow cover and glacier has significant impact on the water and
 energy budgets in TP river basins; it remains a technical challenge to get reliable
 observations due to harsh environment (especially at the basin scale). However,
 recently available satellite-based/LSM-simulated products might provide adequate

characterization of the variation of snow cover and glacier. To quantify the change in snow cover at each basin, we applied the daily cloud free snow composite product from MODIS Terra-Aqua and the Interactive Multisensor Snow and Ice Mapping System for the Tibetan Plateau (Zhang et al., 2012; Yu et al., 2015), in conjunction with the snow water equivalent (SWE) retrieved from Global Snow Monitoring for Climate Research product (GlobSnow-2, <http://www.globsnow.info/>) and the VIC_IGSNRR simulations (Takala et al., 2011; Zhang et al., 2014). We extracted general distribution of glacier of TP from the Second Glacier Inventory Dataset of China (Guo et al., 2014). All gridded datasets used were first uniformly interpolated to a spatial resolution of 0.5 degree based on the bilinear interpolation to make their inter-comparison possible. The datasets were then extracted for each of TP basins.

2.1.4 Monsoon indices

In general, the TP climate is under the influences of the westerlies, Indian summer monsoon and East Asian summer monsoon (Yao et al., 2012). To investigate the changes of monsoon systems and their potential impacts on water budgets in the TP basins, we used three monsoon indices, namely Asian Zonal Circulation Index (AZCI), Indian Ocean Dipole Mode Index (IODMI) and East Asian Summer Monsoon Index (EASMI). Briefly, the IODMI (reflects the dynamics of Indian Summer Monsoon) is an indicator of the east-west temperature gradient across the tropical Indian Ocean (Saji et al., 1999), which can be downloaded from the following website: <http://www.jamstec.go.jp/frcgc/research/d1/iod/HTML/Dipole%20Mode%20Index.html>. The EASMI and AZCI (60°-150°E) reflect the dynamics of East Asian summer monsoon (Li and Zeng, 2002) and the westerlies (represented by Asian Zonal Circulation index), which can be obtained from Beijing Normal University

(<http://ljp.gcess.cn/dct/page/65577>) and the National Climate Center of China
(<http://ncc.cma.gov.cn/Website/index.php?ChannelID=43WCHID=5>), respectively.

2.1.5 Study basins

In this study, we selected 18 river basins of varied sizes (range: 2832-191235 km²; see Table 4-2 for details) with adequate runoff data over a 30-year period (1982-2011). They are distributed in the northwestern, southeastern and eastern parts of the plateau with multiyear-mean and basin-averaged temperature and precipitation ranging from -5.68 to 0.97 °C and 128 to 717 mm, which are solely dominated or under the combined influences of the westerlies, the Indian Summer monsoon and the East Asian monsoon (Yao et al., 2012). There are more glacier and snow covers in the westerlies-dominant basins such as Yerqiang, Yulongkashi and Keliya (10.86-23.27% and 29.16-35.95%, respectively); less for the East Asian monsoon-dominated basins such as Yellow, Yangtze and Bayin (0-0.96% and 9.42-20.05%, respectively) (Table 2).

<Figure 1, here please, thanks>

<Table 2, here please, thanks>

2.2 Methods

2.2.1 Water balance-based ET estimation

The basin-wide water balance at the monthly and annual timescales could be written as the principle of mass conservation (also known as the continuity equation, Oliveira et al., 2014) of basin-wide precipitation (P, mm), evapotranspiration (ET_{wb}, mm), runoff (Q, mm) as well as terrestrial water storage change (ΔS, mm),

$$ET_{wb} = P - Q - \Delta S \quad (1)$$

The terrestrial water storage (ΔS) in Eq. (1) includes the surface, subsurface and ground water changes. It has been demonstrated that ΔS cannot be neglected in water balance calculation over monthly and annual timescales due to snow cover change and anthropogenic interferences (e.g., reservoir operation, agricultural water withdrawal) (Liu et al., 2016a). For the period 2002-2011, we calculated basin-wide ET (ET_{wb}) directly using the GRACE-derived ΔS in Eq. (1). Since GRACE data is absent before 2002, we calculated the monthly ET_{wb} using the following two-step bias-correction procedure (Li X. et al., 2014). We defined $P - Q$ in Eq. (1) as biased ET (ET_{biased} , available from 1982 to 2011) relative to the “true” ET ($ET_{wb} = P - Q - \Delta S$, available during the period 2002-2011 when the GRACE data is available). Over the period 2002-2011, we first fitted ET_{biased} and ET_{wb} series separately using different gamma distributions, which has been evidenced as an proper method for modeling the probability distribution of ET (Bouraoui et al., 1999). The monthly ET_{biased} series (2002-2011) can then be bias-corrected through the inverse function (F^{-1}) of the gamma cumulative distribution function (CDF, F) of ET_{wb} by matching the cumulative probabilities between two CDFs as follow (Liu et al., 2016a),

$$ET_{corrected}(m) = F^{-1}(F(ET_{biased}(m)|\alpha_{biased}, \beta_{biased})|\alpha_{wb}, \beta_{wb}) \quad (2)$$

Here α_{biased} , β_{biased} and α_{wb} , β_{wb} are shape and scale parameters of gamma distributions for ET_{biased} and ET_{wb} . $ET_{corrected}(m)$ and $ET_{biased}(m)$ represent the monthly corrected and biased ET, respectively. The bias correction procedure can be flexibly applied to the period 1983-2011 by matching the CDF of ET_{biased} (1983-2011) to that of $ET_{corrected}$ (2002-2011). The second step of bias correction is to eliminate the annual bias through the ratio of annual ET_{biased} to annual $ET_{corrected}$ calculated in the first step using the following method,

$$ET_{\text{final}}(m) = \frac{ET_{\text{biased}}(a)}{ET_{\text{corrected}}(a)} \times ET_{\text{corrected}}(m) \quad (3)$$

where $ET_{\text{final}}(m)$ is the final monthly ET after bias correction. $ET_{\text{biased}}(a)$ and $ET_{\text{corrected}}(a)$ represent the annual biased and corrected ET while $ET_{\text{corrected}}(m)$ is the monthly corrected ET obtained from the first step. The procedure was then applied to correct the monthly ET_{biased} series and calculated the monthly $ET_{\text{corrected}}$ during the period 1982-2001 for all TP basins. We take these results as sufficient representation of the “true” ET (ET_{wb}) for evaluating multiple ET products and trend analysis.”

277

2.2.2 Modified Mann-Kendall test method

The Mann-Kendall (MK) test is a rank-based nonparametric approach which is less sensitive to outlier relative to other parametric statistics, but it is sometimes influenced by the serial correlation of time series. Pre-whitening is often used to eliminate the influence of lag-1 autocorrelation before the use of MK test. For example, $X(X_1, X_2, \dots, X_n)$ is a time series data, it will be replaced by $(X_2 - cX_1, X_3 - cX_2, \dots, X_{n+1} - cX_n)$ in pre-whitening if the lag-1 autocorrelation coefficient (c) is larger than 0.1 (von Storch, 1995). However, significant lag-1 autocorrelation may still be detected after pre-whitening because only the lag-1 autocorrelation is considered in pre-whitening (Zhang et al., 2013). Moreover, it sometimes underestimate the trend for a given time series (Yue et al., 2002). Hamed and Rao (1998) proposed a modified version of MK test (MMK) to consider the lag- i autocorrelation and related robustness of the autocorrelation through the use of equivalent sample size, which has been widely used in previous studies during the last five decades (McVicar et al., 2012; Zhang et al., 2013; Liu and Sun, 2016). In the MMK approach, if the lag- i autocorrelation coefficients are significantly distinct from

zero, the original variance of MK statistics will be replaced by the modified one. In this study, we used the MMK approach to quantify the trends of water budget components in 18 TP basins and the significance of trend was tested at the >95% confidence level.

2.2.3 Uncertainty analysis

~~The uncertainty associated multi-source dataset used (no observation or the observations are not adequate at the basin scale) for quantifying the dynamics of certain water budget components (i.e., ET and precipitation) are also analyzed. We investigate the seasonal cycles and trends of these components by using different datasets together in the analysis to show the potential uncertainties in this study.~~

3 Results and Discussion

3.1 ET evaluation and General hydrological characteristics of 18 TP basins

We first assessed the VIC_IGSNRR simulated runoff against the observations for each basin (for example, at Tangnaihaid and Pangduo stations in Fig.2). If the Nash Efficiency coefficient (NSE) between the observation and simulation is above 0.65, the VIC_IGSNRR simulated runoff is acceptable and could be used to replace the missing runoff values for a given basin. Moreover, the CMA precipitation is consistent with TRMM (Corr = 0.86, RMSE = 8.34 mm/month) and IGSNRR forcing (Corr = 0.94, RMSE = 7.15mm/month) precipitation for multiple basins (i.e., for the smallest basin above Tongren station, Fig.2). Moreover, the magnitudes of GRACE-derived annual mean water storage change (ΔS) in 18 TP basins are relatively less than those for other water balance components such as annual P, Q and ET (Table 2 and Table 3). The uncertainties among GRACE-derived annual mean ΔS

from different data processing centers (CSR, GFZ and JPL) are small for 18 basins except for the basins controlled by Gadatan and Tangnaihahai stations.

< Figure 2, here please, thanks>

< Table 3, here please, thanks>

We then evaluated six ET products in 18 TP basins against our calculated ET_{wb} at a monthly basis during the period 1983-2006 (Fig. 3). The ranges of monthly averaged ET among different basins (approximately 4–39 ~~mm~~mm/month⁺) are very close for all products compare to that calculated from the ET_{wb} (6–42 ~~mm~~mm/month⁺). However, GLEAM_E (correlation coefficient: Corr = 0.85 and root-mean-square-error: RMSE = 5.69 ~~mm~~mm/month⁺) and VIC_E (Corr = 0.82 and RMSE = 6.16 ~~mm~~mm/month⁺) perform relatively better than others. Although Zhang_E and GNoah_E were found closely correlated to monthly ET_{wb} in the upper Yellow River, the upper Yangtze River, Qiangtang and Qaidam basins (Li X. et al., 2014), they did not exhibit overall good performances (Corr = 0.61, RMSE = 7.97 ~~mm~~mm/month⁺ for Zhang_E and Corr = 0.42, RMSE = 10.16 ~~mm~~mm/month⁺ for GNoah_E) for 18 TP basin used in this study. We thus use GLEAM_E and VIC_E together with ET_{wb} to analyze the seasonal cycles and trends of ET in 18 TP basins in the following sections.

< Figure 3, here please, thanks>

To investigate the general hydroclimatic characteristics of river basins over the TP, we classify 18 basins into three categories, namely westerlies-dominated basins (Yerqiang, Yulongkashi and Kelia), Indian monsoon-dominated basins (Brahmaputra and Salween), and East Asian monsoon-dominated basins (Yellow, Yalong and Yangtze) referred to Tian et al. (2007), Yao et al. (2012) and Dong et al. (2016). Interestingly, they are clustered into three groups under Budyko framework (Budyko,

1974; Zhang D. et al., 2016) with relatively lower evaporative index in Indian monsoon-dominant basins and higher aridity index in westerlies-dominant basins, which reveal various long-term hydroclimatologic conditions (Fig. 4). Overall, from the westerlies-dominant, Indian monsoon-dominant to East Asian monsoon-dominant basins, the annual mean air temperature (-5.68 -0.97 °C) and ET (and thus runoff coefficient gradually decreases) increases ~~(-5.68 -0.97 °C) while while the~~ multiyear mean glacier area (and thus the glacier melt normalized by precipitation) gradually decreases (23.27 ~ 0%) gradually from the westerlies dominant, Indian monsoon dominant to East Asian monsoon dominant basins. The vegetation status (NDVI range: 0.05 -0.43; LAI range: 0.03 -0.83) tends to be better and ET increases (and thus runoff coefficient gradually decreases) from cold to warm basins (Fig. 4 and Table 42). Moreover, the vegetation status (NDVI range: 0.05-0.43; LAI range: 0.03-0.83) tends to be better. ~~The R² between basin-averaged NDVI and ET is (-0.76) is much higher than that between T and NDVI (0.35), which indicating that the water availability plays a more important role than the heat stress (i.e., colder status) over such basins. which shows a clear vegetation control on ET in 18 TP basins.~~ The results are in line with Shen et al. (2015), which indicated that the spatial pattern of ET trend was significantly and positively correlated with NDVI trend over the TP. The dominant climate systems are overall discrepant for the three TP regions with different water-energy characteristics and sources of water vapor. For example, in the westerlies-controlled basins, more glaciers developed due to their relatively colder air temperature and special seasonality of precipitation. Therefore, there are more snow melt contributions to total river streamflow with global warming during the period 1983-2006. ~~The westerlies-controlled basins are relatively colder than the Indian monsoon-dominated basins, thus they develop more glaciers (and thus have more~~

带格式的: 字体颜色: 自动设置

带格式的: 字体颜色: 红色

~~snow melt contributions to total river streamflow) and have relatively less vegetation (and thus limit vegetation transpiration)~~ It is a general picture of hydrological regime in high-altitude and cold regions (Zhang et al., 2013; Cuo et al., 2014), which could be interpreted from the perspective of multi-source datasets in the data-sparse TP.

< Figure 4, here please, thanks>

3.2 Seasonal cycles of basin-wide water budget components for the TP basins

The multi-year means of water budget components (i.e., P, Q, ET, snow cover and SWE) and vegetation parameters (i.e., NDVI and LAI) are calculated for each calendar month and for 18 TP river basins using multi-source datasets available from 1982 to 2011. Overall, the seasonal variations of P, Q, ET, air temperature and vegetation parameters are similar in all TP basins with peak values occurred in May to September (Fig.5 and Fig.6). The seasonal cycles of snow cover and SWE are generally consistent among the basins (the peak values mainly occur from October to next April, Fig.7). With the ascending air temperature from cold to warm months, the basin-wide precipitation increases and vegetation cover expands gradually (the basin-wide ET also increase). Meanwhile, snow cover and glaciers retreat gradually with the melt water supplying the river discharge together with precipitation. The inter-basin variations of hydrological regime are to a large extent linked to the climate systems that prevail over the TP.

< Figure 5, here please, thanks>

Although the temporal patterns of hydrological components are generally analogous, they vary among the parameters, climate zones and even basins (Zhou et al., 2005). For example, relative to air temperature, the seasonal pattern of runoff is similar to

precipitation which reveals that runoff is mainly controlled by precipitation in most TP basins. It is in agreement with that summarized by Cuo et al. (2014). In the westerlies-dominated basins, the peak values of precipitation and runoff mainly concentrate in June-August, which contribute approximately 68-82% and 67-78% of annual totals, respectively. During this period, the runoff always exceeds precipitation which indicates large contributions of glacier/snow-melt water to streamflow. It is consistent with the existing findings in Tarim River (Yerqiang, Yulongkashi and Keliya rivers are the major tributaries of Tarim River), which indicated that the melt water accounted for about half of the annual total streamflow (Fu et al., 2008). The ET (vegetation cover) in three westerlies-dominated basins are relatively less (scarcer) than that in other TP basins while the percentages of glacier and seasonal snow cover are higher in these basins which contribute more melt water to river discharge (Fig.6 and Fig.7). Overall, the SWE in Yerqiang, Yulongkashi and Keliya rivers are higher in winter than other seasons, but they vary with basins and products which reflect considerable uncertainties in SWE estimations.

< Figure 6, here please, thanks>

In the Indian monsoon and East Asian monsoon dominated basins, the runoff concentrates during June-September (or June- October) with precipitation being the dominant contributor of annual total runoff. For example, the peak values of precipitation and runoff occur during June-September at Zhimenda station (contributing about 80% and 74% of the annual totals) while those occur during June-October at Tangnaihai station (contributing about 78% and 71% of the annual totals, respectively). The results are quite similar to the related studies in eastern and southern TP such as Liu (1999), Dong et al. (2007), Zhu et al. (2011), Zhang et al. (2013), Cuo et al. (2014). The vegetation cover (ET) in most basins is denser (higher)

than that in the westerlies-dominant basins. Moreover, the seasonal snow mainly covers from mid-autumn to spring and correspondingly the SWE is relatively higher in these months in all basins except for Yellow River above Xining station, Salween River above Jiayuqiao station and Brahmaputra River above Nuxia and Yangcun stations.

< Figure 7, here please, thanks>

3.3 Trends of basin-wide water budget components for the TP basins

The Q, P and ET_{wb} all ascended under regional warming during the past 30 years in the westerlies-dominated basins (Fig.8), except for P in the Yerqiang River basin (Kulukelangan station). The aridity index (PET/P), which is an indicator for the degree of dryness, slightly declined in all basins in northwestern TP. Although both P and PET ~~were found~~ increased in the Keliya River basin since the 1980s (Shi et al., 2003; Yao et al., 2014), the ~~declined~~ PET/P declined due to the higher rates of the increase of P than that of PET. is, to some extent, attributed to the ascending P exceed the increase in PET. The climate moistening (Shi et al., 2003) in the headwaters of these inland rivers would be beneficial to the water resources and oasis agro-ecosystems in the middle and lower basins. The increase in streamflow was also found in most tributaries of the Tarim River (Sun et al., 2006; Fu et al., 2010; Mamat et al., 2010). Moreover, the westerlies, revealed by the Asian Zonal Circulation Index (60° - 150° E), slightly enhanced (linear trend: 0.21) over the period 1982-2011 (Fig.9). With the strengthening westerlies, more water vapor may be transported and fell as ~~precipitation-rain~~ or snow in northwestern TP (e.g., the eastern Pamir region). Both SWE products (VIC_IGSNRR simulated and GlobaSnow-2 product) showed slightly increase across these basins with rising seasonal snow covers and glaciers (Yao et al., 2012). More precipitation was transformed into snow /glacier and the runoff

coefficient (Q/P) exhibited decrease with precipitation obviously increased (Fig.8). In addition, the transpiration in these basins might decrease with vegetation degradation as revealed by the NDVI and LAI (Yin et al., 2016) but the atmospheric evaporative demand indicated by CRU PET increased (significantly increase in the Yulongkashi and Keliya rivers) during the period 1982-2011.

< Figure 8, here please, thanks>

< Figure 9, here please, thanks>

In the East Asian monsoon dominated basins, there are two types of change for basin-wide water budget components. For example, P and Q slightly decreased in the upper Yellow River (Tangnihai, Huangheyan and Jimai stations) and Yalong River (Yajiang station) but increased in other basins (Zelingou, Gandatan, Xining, Tongren and Zhimenda stations) over the period of 1982-2011 (Fig.10). The declined Q and P in the upper Yellow and Yalong Rivers (located at the eastern Tibetan Plateau) were consistent with that found by Cuo et al. (2013, 2014) and Yang et al. (2014), and were in line with the weakening East Asian Summer Monsoon (linear slope: -0.01) (Fig.9). The vegetation turned green while ET_{wb} and PET increased in all East Asian monsoon dominated basins (except for ET_{wb} in the basins above Tongren and Yajiang stations) with the significantly ascending air temperature during the period 1982-2011. The aridity index (PET/P) decreased in all basins except for the upper Yellow River basin above Jimai station and the upper Yalong River basin above Yajiang station. Moreover, both the runoff coefficients and SWE decreased except for the Bayin River above Zelingou station and the upper Yellow River above Tongren station in the East Asian monsoon dominated basins.

< Figure 10, here please, thanks>

The P , ET_{wb} and Q also increased in the Indian monsoon-dominated basins (except

for ET_{wb} in the basin above Yangcun station) such as Salween River and Brahmaputra River (Fig.11), which are in line with the strengthening (linear trend: 0.01) of the Indian summer monsoon (revealed by the Indian Ocean Dipole Mode Index) during the specific period 1982-2011 (Fig.9). For example, at Jiayuqiao station, the annual streamflow showed a slightly increasing trend which was consistent with that examined by Yao et al. (2012) during the period 1980-2000. The vegetation status, revealed by NDVI and LAI, turned better ~~asseeiated~~associated with the ascending air temperature. The aridity index (PET/P) decreased in all basins except for the Brahmaputra River above Tangjia station, which indicated that most basins in the Indian monsoon-dominated regions turned wetter over the period of 1982-2011. The increased PET/P in Brahmaputra River basin may be consistent with the drying moisture flux in the southeastern TP, as illustrated by by Gao et al. (2014). The runoff coefficient (Q/P) increased at Gongbujiangda and Nuxia while decreased at Jiayuqiao, Pangduo, Tangji and Yangcun stations. Moreover, the basin-wide SWE declined in the upper Salween River and Brahmaputra River above Pangduo, Tangjia and Gongbujiangda stations while increased in Brahmaputra River above Nuxia and Yangcun stations.

< Figure 11, here please, thanks>

3.4 Uncertainties

The results may unavoidably associate with some uncertainties inherited from the multi-source datasets used. The primary sources of uncertainty may arise from the precipitation inputs. We compared the seasonal cycles and annual trends in different precipitation products, i.e. CMA_P, IGSNRR_P and TRMM_P (and their calculated ET_{wb} from the water balance) during the period 2000-2011 (Fig. 12 and Fig. 13). We found there are some uncertainties among different precipitation

products and thus among their estimated ET_{wb} , especially in the westerlies-dominated basins. However, for each basin, the seasonal cycles of precipitation (and their calculated ET_{wb}) calculated from different products are overall similar (especially for the observation-based products, CMA_P and IGSNNR_P). The signs of trend for annual CMA_P and IGSNNR_P (and their calculated ET_{wb}) are consistent in most river basins (i.e., 14 out 18 basins for two precipitation products and 17 out 18 basins for their calculated ET_{wb}) during the period 1982-2011. The consistency of trends between two precipitation products, to some extent, revealed that the trends in CMA_P were not obviously influenced by the changing density of rain gauges in TP basins. Although some uncertainties exist due to limited and unevenly distributed meteorological stations used in the plateau and the influences of complex terrain, CMA_P is still the best observation-based precipitation product nowadays in China which could be applied to hydrological studies in the TP.

< Figure 12, here please, thanks>

< Figure 13, here please, thanks>

Although the seasonal cycles of ET_{wb} could be captured by GLEAM_E and VIC_E, they still have considerable uncertainties at some stations (e.g., Numaitilangan, Gongbujiangda and Nuxia) (Fig.5). Compared to the annual trend of ET_{wb} (Table 4), most ET products (including the well-performed GLEAM_E and VIC_E) could not detect the decreasing trends in 7 out of 18 basins (Kulukelangan, Tongguziluoke, Xining, Tongren, Jimai, Nuxia and Gongbujiangda) due to their different forcing data, algorithm used as well as varied spatial-temporal resolutions (Xue et al., 2013; Li et al., 2014; Liu et al., 2016a). In particular, it is well known that land surface models have some difficulties (e.g., parameter tuning in boundary layer schemes) when applying to the TP, even though they sometimes have good performances in different

regions/basins (Xia et al., 2012; Bai et al., 2016). For example, Xue et al. (2013) indicated that GNoah_E underestimated the ET_{wb} in the upper Yellow River and Yangtze River basins on the Tibetan Plateau mainly due to its negative-biased precipitation forcing. We thus only used ET_{wb} in the trend detection of water budget components in Fig.8, Fig.10 and Fig.11 in this study. The two SWE products also showed large uncertainty with respect to both their seasonal cycles and trends. The VIC_IGSNRR simulated and GlobaSnow-2 SWEs have not been validated in the TP due to the lack of snow water equivalent observations, but in some basins (e.g., Zelingou and Numaitilangan) they showed similar seasonal cycles and annual trends.

<Table 4, here please, thanks>

The interpolation of missing values of runoff with VIC_IGSNRR simulated runoff and the gridded precipitation data (which interpolated from limited gauged precipitation over the plateau) also introduced uncertainties. There are also considerable uncertainties arising from empirical extending the ET series back prior to the GRACE era. However, the trends in ET_{wb} have not significantly affected by erroneous trends in the precipitation inputs to the bias-correction based water balance calculation. For example, the trends in CMA_P and IGSNRR_P are opposite in few basins (No. 01, 07, 08, 13 in Fig. 13), but the trends in their calculated ET_{wb} are both consistent for each basin. It is, to some extent, certified the effectiveness of the bias correction-based ET-estimate approach. With these caveats, we can interpret the general hydrological regimes and their responses to the changing climate in the TP basins from solely the perspective of multi-source datasets, which are comparable to the existing studies based on the in situ observations and complex hydrological modeling.

4 Summary

In this study, we investigated the seasonal cycles and trends of water budget components in 18 TP basins during the period 1982-2011, which is not well understood so far due to the lack of adequate observations in the harsh environment, through integrating the multi-source global/regional datasets such as gauge data, satellite remote sensing and land surface model simulations. By using a two-step bias correction procedure, we calculated the annual basin-wide ET_{wb} through the water balance approach considering the impacts of ~~glacier and~~ water storage change. We found that the GLEAM_E and VIC_E perform better relative to other products against the calculated ET_{wb} .

From the Budyko framework perspective, the general water and energy budgets are different in the westerlies-dominated (with higher aridity index, runoff coefficient and glacier cover), the Indian monsoon-dominated and the East Asian monsoon-dominated (with higher air temperature, vegetation cover and evapotranspiration) basins. In the 18 TP basins, precipitation is the major contributor to the river runoff, which concentrates mainly during June-October (June-August for the westerlies-dominated basins, June-September or June to October for the Indian monsoon-dominated and the East Asian monsoon-dominated basins). The basin-wide SWE is relatively high from mid-autumn to spring for all 18 TP basins except for Keliya River and Brahmaputra River above the Nuxia and Yangcun stations. The vegetation cover is relatively less whereas snow/glacier cover is more in the westerlies-dominant basins compared to other basins. During the period 1982-2011, we found that the P, Q and ET_{wb} increased across most of the basins in Tibetan Plateau ~~with the exception of ;receded at~~ some tributaries located at the upper Yellow

River and Yalong River due to the weakening East Asian monsoon. The aridity index (PET/P) exhibited a decrease trend in most TP basins which ~~corresponded~~ corresponds to the warming and moistening climate in the TP and western China. Moreover, the runoff coefficient (Q/P) declined in most basins which may be, to some extent, due to ET increase induced by vegetation greening and the influences of snow and glacier changes. Although there are considerable uncertainties inherited from multi-source data used, the general hydrological regimes in the TP basins could be revealed, which are consistent to the existing results obtained from in situ observations and complex land surface modeling. It ~~indicated~~ indicates the usefulness of integrating the multiple datasets (e.g., in situ observations, remote sensing-based products, reanalysis outputs, land surface model simulations and climate model outputs) for hydrological applications. The generalization here could be helpful for understanding the hydrological cycle and supporting sustainable water resources management and eco-environment protection in the Tibetan Plateau ~~under global~~ warming.

Author contributions. Wenbin Liu and Fubao Sun developed the idea to see the general water budgets in the TP basins from the perspective of multisource datasets. Wenbin Liu collected and processed the multiple datasets with the help of Yanzhong Li, Guoqing Zhang, Wee Ho Lim, Hong Wang as well as Peng Bai, and prepared the manuscript. The results were extensively commented and discussed by Fubao Sun, Jiahong Liu and Yan-Fang Sang.

Acknowledgements. This study was supported by the National Key Research and Development Program of China (2016YFC0401401 and 2016YFA0602402), National Natural Science Foundation of China (41401037 and 41330529), the Open Research

Fund of State Key Laboratory of Desert and Oasis Ecology in Xinjiang Institute of Ecology and Geography, Chinese Academy of Sciences (CAS), the CAS Pioneer Hundred Talents Program (Fubao Sun), the CAS President's International Fellowship Initiative (2017PC0068) and the program for the "Bingwei" Excellent Talents from the Institute of Geographic Sciences and Natural Resources Research, CAS. We are grateful to the NASA MEaSUREs Program (Sean Swenson) for providing the GRACE land data processing algorithm. The basin-wide water budget series in the TP Rivers used in this study are available from the authors upon request (liuwb@igsnr.ac.cn). We thank the editors and reviewers for their invaluable comments and constructive suggestions.

References

- Akhtar, M., Ahmad, N., and Booij, M.J.: Use of regional climate model simulations as input for hydrological models for the Hindukush-Karakorum-Himalaya region, *Hydrol. Earth Syst. Sci.* 13, 1075-1089, 2009.
- Bai, P., Liu, X.M., Yang, T.T., Liang, K., and Liu, C.M.: Evaluation of streamflow simulation results of land surface models in GLDAS on the Tibetan Plateau, *J. Geophys. Res. Atmos.*, 121, 12180-12197, 2016.
- Berrisford, P, Lee, D., Poli, P., Brugge, R., Fielding, K., Fuentes, M., Kallberg, P., Kobayashi, S., Uppala, S., and Simmons, A.: The ERA-interim archive. ERA Reports Series No. 1 Version 2.0, Available from: <https://www.researchgate.net/publication/41571692_The_ERA-interim_archive>, 2011.
- Bookhagen, B. and Burbank, D.W.: Toward a complete Himalayan hydrological budget: spatiotemporal distribution of snowmelt and rainfall and their impact on river discharge, *J. Geophys. Res.*, 115, F03019, 2010.
- Bouraoui, F., Vachaud, G., Li, L.Z.X., LeTreut, H., and Chen, T.: Evaluation of the impact of climate changes on water storage and groundwater recharge at the watershed scale, *Clim. Dyn.*, 15(2), 153-161, 1999.

Budyko, M.I.: Climate and life. Academic Press, 1974.

Chen, D., Xu, B., Yao, T., Guo, Z., Cui, P., Chen, F., Zhang, R., Zhang, X., Zhang, Y., Fan, J., Hou, Z., and Zhang, T.: Assessment of past, present and future environmental changes on the Tibetan Plateau, Chinese SCI. Bull., 60(32), 3025-3035, 2015 (in Chinese).

Cuo, L., Zhang, Y.X., Bohn, T.J., Zhao, L., Li, J.L., Liu, Q.M., and Zhou, B.R.: Frozen soil degradation and its effects on surface hydrology in the northern Tibetan Plateau, J. Geophys. Res. Atmos., 120(6), 8276-8298, 2015.

Cuo, L., Zhang, Y.X., Gao, Y., Hao, Z., and Cairang, L.: The impacts of climate change and land cover/use transition on the hydrology in the upper Yellow River Basin, China, J. Hydrol., 502, 37-52, 2013.

Cuo, L., Zhang, Y.X., Zhu, F.X., and Liang, L.Q.: Characteristics and changes of streamflow on the Tibetan Plateau: A review, J. Hydrol. Reg. stud., 2, 49-68, 2014.

Dong, X., Yao, Z., and Chen, C.: Runoff variation and responses to precipitation in the source regions of the Yellow River, Resour. Sci., 29(3), 67-73, 2007 (in Chinese).

Dong, W., Lin, Y., Wright, J.S., Ming, Y., Xie, Y., Wang, B., Luo, Y., Huang, W., Huang, J., Wang, L., Tian, L., Peng, Y., and Xu, F.: Summer rainfall over the southwestern Tibetan Plateau controlled by deep convection over the Indian Subcontinent, Nat. Commun., 7, 10925, 2016.

Duan, A.M. and Wu, G.X.: Change of cloud amount and the climate warming on the Tibetan Plateau, Geophys. Res. Lett., 33, L22704, 2006.

Fu, L., Chen, Y., Li, W., Xu, C., and He, B.: Influence of climate change on runoff and water resources in the headwaters of the Tarim River, Arid Land Geogr., 31(2), 237-242, 2008 (in Chinese).

Fu, L., Chen, Y., Li, W., He, B., and Xu, C.: Relation between climate change and runoff volume in the headwaters of the Tarim River during the last 50 years., J. Desert Res., 30(1), 204-209, 2010 (in Chinese).

Gao, Y.H., Cuo, L., and Zhang, Y.X.: Changes in moisture flux over the Tibetan Plateau during 1979-2011 and possible mechanisms, J. Climate, 27, 1876-1893, 2014.

Guo, W.Q., Liu, S.Y., Yao, X.J., Xu, J.L., Shangguan, D.H., Wu, L.Z., Zhao, J.D., Liu, Q., Jiang, Z.L., Wei, J.F., Bao, E.J., Yu, P.C., Ding, L.F., Li, G., Ge, C.M., and Wang, Y.: The Second Glacier Inventory Dataset of China, Cold and Arid Regions Science Data Center at Lanzhou,

doi: 10.3972/glacier.001.2013.db, 2014.

Hamed, K.H. and Rao, A.R.: A modified Mann-Kendall trend test for autocorrelation data, J.Hydrol., 204(1-4), 182-196, 1998.

Huffman, G.J., E.F., Bolvin, D.T., Nelkin, E.J., and Adler, R.F.: last updated 2013: TRMM Version 7 3B42 and 3B43 Data Sets, NASA/GSFC, Greenbelt, MD. Data set accessed at <http://mirador.gsfc.nasa.gov/cgi-bin/mirador/presentNavigation.pl?tree=project&project=TRMM&dataGroup=Gridded&CGIS ESSID=5d12e2ffa38ca2aac6262202a79d882a>, 2012.

Harris, I., Jones, P.D., Osborn, T.J., and Lister, D.H.: Updated high-resolution grids of monthly climatic observations – the CRU TS3.10 Dataset, Int. J. Climatol., 34 (3), 623-642, 2014.

Immerzeel, W.W., van Beek, L.P.H., and Bierkens, M.F.P.: Climate change will affect the Asian water towers, Science, 328, 1382-1385, 2010.

Jung, M., Reichstein, M., Ciais, P., Seneviratne, S.I., Sheffield, J., Goulden, M.L., Bonan, G., Cescatti, A., Chen, J., de Jeu, R., Dolman, A.J., Eugster, W., Gerten, D., Gianelle, D., Gobron, N., Heinke, J., Kimball, J., Law, B.E., Montagnani, L., Mu, Q., Mueller, B., Oleson, K., Papale, D., Richardson, A.D., Rouspard, O., Running, S., Tomelleri, E., Viovy, N., Weber, U., Williams, C., Wood, E., Zaehle, S., and Zhang, K.: Recent decline in the global land evapotranspiration trend due to limited moisture supply, Nature, 467, 951-954, 2010.

Kobayashi, S., Ota, Y., Harada, Y., Ebata, A., Moriya, M., Onoda, H., Onogi, K., kamahori, H., kobayashi, C., Endo, H., miyaoka, K., and Takahashi, K.: The JRA-55 Reanalysis: General specifications and basic characteristics, J.Meteor. Soc. Japan, 93(1), 5-58, doi: 10.2151/jmsj.2015-001, 2015.

Landerer, F.W. and Swenson, S.C.: Accuracy of scaled GRACE terrestrial water storage estimates, Water Resour.Res., 48, W04531, 2012.

Li, F.P., Zhang, Y.Q., Xu, Z.X., Liu, C.M., Zhou, Y.C., and Liu, W.F.: Runoff predictions in ungauged catchments in southeast Tibetan Plateau, J. Hydrol., 511, 28-38, 2014.

Li, F.P., Zhang, Y.Q., Xu, Z.X., Teng, J., Liu, C.M., Liu, W.F., and Mpelasoka, F.: The impact of climate change on runoff in the southeastern Tibetan Plateau, J. Hydrol., 505, 188-201, 2013.

681 Li, J.P. and Zeng, Q.C.: A unified monsoon index, *Geophys. Res. Lett.*, 29(8), 1274, 2002.

682 Li, X.P., Wang, L., Chen, D.L., Yang, K., and Wang, A.H.: Seasonal evapotranspiration changes
683 (1983-2006) of four large basins on the Tibetan Plateau, *J. Geophys. Res.*, 119 (23),
684 13079-13095, 2014.

685 Liang, S.L. and Xiao, Z.Q.: Global Land Surface Products: Leaf Area Index Product Data
686 Collection(1985-2010), Beijing Normal University, doi:10.6050/glass863.3004.db, 2012.

687 Liu, T.: Hydrological characteristics of Yalungzangbo River, *Acta Geogr. Sin.*, 54 (Suppl.),
688 157-164, 1999 (in Chinese).

689 Liu, W.B. and Sun, F.B.: Assessing estimates of evaporative demand in climate models using
690 observed pan evaporation over China, *J. Geophys. Res. Atmos.*, 121, 8329-8349, 2016.

691 Liu, W.B., Wang, L., Zhou, J., Li, Y.Z., Sun, F.B., Fu, G.B., Li, X.P., and Sang, Y-F.: A worldwide
692 evaluation of basin-scale evapotranspiration estimates against the water balance method, *J.*
693 *Hydrol.*, 538, 82-95, 2016a.

694 Liu, W.B., Wang, L., Chen, D.L., Tu, K., Ruan, C.Q., and Hu, Z.Y.: Large-scale circulation
695 classification and its links to observed precipitation in the eastern and central Tibetan Plateau,
696 *Clim. Dyn.*, 46, 3481-3497, 2016b.

697 Liu, X.M., Yang, T., Hsu, K., Liu, C., and Sorooshian, S.: Evaluating the streamflow simulation
698 capability of PERSIANN-CDR daily rainfall products in two river basins on the Tibetan Plateau,
699 *Hydrol. Earth Syst. Sci.*, 21, 169-181, 2017.

700 Long, D., Shen, Y.J., Sun, A., Hong, Y., Longuevergne, L., Yang, Y.T., Li, B., and Chen, L.:
701 Drought and flood monitoring for a large karst plateau in Southwest China using extended
702 GRACE data, *Remote Sens. Environ.*, 155, 145-160, 2014.

703 Lucchesi, R.: File specification for MERRA products, GMAO Office Note No.1 (version 2.3), 82
704 pp, available from http://gmao.gsfc.nasa.gov/pubs/office_notes, 2012.

705 Ma, N., Szilagyi, J., Niu, G.Y., Zhang, Y.S., Zhang, T., Wang, B.B., and Wu, Y.H.: Evaporation
706 variability of Nam Co Lake in the Tibetan Plateau and its role in recent rapid lake expansion, *J.*
707 *Hydrol.*, 537, 27-35, 2016.

708 Ma, N., Zhang, Y.S., Guo, Y.H., Gao, H.F., Zhang, H.B., and Wang, Y.F.: Environmental and
28 / 56

709 biophysical controls on the evapotranspiration over the highest alpine steppe, *J. Hydrol.*, 529,
710 980-992, 2015.

711 Mamat, A., Halik, W., and Yang, X.: The climatic changes of Qarqan river basin and its impact on
712 the runoff, *Xinjiang Agric. Sci.*, 47 (5), 996-1001, 2010 (in Chinese).

713 McVicar, T.R., Roderick, M., Donohue, R.J., Li, L.T., Van Niel, T.G., Thomas, A., Grieser, J.,
714 Jhajharia, D., Himri, Y., Mahowald, N.M., Mescherskaya, A.V., Kruger, A.C., Rehman, S., and
715 Dinpashoh, Y.: Global review and synthesis of trends in observed terrestrial near-surface wind
716 speeds: implications for evaporation, *J. Hydrol.*, 416-417, 182-205, 2012.

717 Miralles, D.G., De Jeu, R.A.M., Gash, J.H., Holmes, T.R.H., and Dolman, A.J.: Magnitude and
718 variability of land evaporation and its components at the global scale, *Hydrol. Earth Syst. Sci.*, 15,
719 967-981, 2011.

720 Miralles, D.G., Gash, J.H., Holmes, T.R.H., de Jeu, R.A.M., and Dolman, A.J.: Global canopy
721 interception from satellite observations, *J. Geophys. Res.*, 115, D16122, 2010.

722 Oliveira, P.T.S., Mearing, M.A., Moran, M.S., Goodrich, D.C., Wendland, E., and Gupta, H.V.:
723 Trends in water balance components across the Brazilian Cerrado, *Water Resour. Res.*, 50,
724 7100-7114, 2014.

725 Rodell, M., Houser, P.R., Jambor, U., Gottschalk, J., Mitchell, K., Meng, C.-J., Arsenault, K.,
726 Cosgrove, B., Radakovich, J., Bosilovich, M., Entin, J.K., Walker, P., Lohmann, D., and Toll, D.:
727 The global land data assimilation system, *B. Am. Meteorol. Soc.*, 85, 381-394, 2004.

728 Rui, H.: README Document for Global Land Data Assimilation System Version 2 (GLDAS-2)
729 Products, GES DISC, 2011.

730 Saji, N.H., Goswami, B.N., Vinayachandran, P.N., and Yamagata, T.: A dipole mode in the tropical
731 Indian Ocean, *Nature*, 401, 360-363, 1999.

732 Shen, M.G., Piao, S.L., Jeong, S., Zhou, L.M., Zeng, Z.Z., Ciais, P., Chen, D.L., Huang, M.T., Jin,
733 C.S., Li, L.Z.X., Li, Y., Myneni, R.B., Yang, K., Zhang, G.X., Zhang, Y.J., and Yao, T.D.:
734 Evaporative cooling over the Tibetan Plateau induced by vegetation growth, *Proc. Natl. Acad.*
735 *Sci. U. S.A.*, 112(30), 9299-9304, 2015.

736 Shi, Y.F., Shen, Y.P., Li, D.L., Zhang, G.W., Ding, Y.J., Hu, R.J., and Kang, E.S.: Discussion on
737 the present climate change from Warm2dry to Warm2wet in northwest China, *Quat. Sci.*, 23(2),
738 152-164, 2003 (in Chinese).

739 Shepard, D.S.: Computer mapping: the SYMAP interpolation algorithm. *Spatial Statistics and*
740 *Models*, G.L. Gaile and C.J. Willmott, Eds., D. Reidel, 133-145, 1984.

741 Sun, B., Mao, W., Feng, Y., Chang, T., Zhang, L., and Zhao, L.: Study on the change of air
742 temperature, precipitation and runoff volume in the Yarkant River basin, *Arid Zone Res.*, 23(2),
743 203-209, 2006 (in Chinese).

744 Takala, M., Luojus, K., Pulliainen, J., Derksen, C., Lemmetyinen, J., Kärnä J.-P., Koskinen, J., and
745 Bojkov, B.: Estimating northern hemisphere snow water equivalent for climate research through
746 assimilation of spaceborne radiometer data and ground-based measurements, *Remote*
747 *Sens. Environ.*, 115 (12), 3517-3529, 2011.

748 Tapley, B.D., Bettadpur, S., Watkins, M., and Reigber, C.: The gravity recovery and climate
749 experiment: mission overview and early results, *Geophys. Res. Lett.*, 31, L09607, 2004.

750 Tian, L., Yao, T., MacClune, K., White, J.W.C., Schilla, A., Vaughn, B., Vachon, R., and
751 Ichiyanagi, K.: Stable isotopic variations in west China: a consideration of moisture sources, *J.*
752 *Geophys. Res. Atmos.*, 112, D10112, 2007.

753 Tucker, C.J., Pinzon, J.E., Brown, M.E., Slayback, D., Pak, E.W., Mahoney, R., Vermote, E., and
754 El Saleous, N.: An extended AVHRR 8 km NDVI data set compatible with MODIS and SPOT
755 vegetation NDVI data, *Int. J. Remote Sens.*, 26(20), 4485-4498, 2005.

756 von Storch, H.: Misuses of statistical analysis in climate research, In *Analysis of Climate*
757 *Variability: Applications of Statistical Techniques*, Springer-Verlag: Berlin, 11-26, 1995.

758 Wang, A. and Zeng, X.: Evaluation of multireanalysis products within site observations over the
759 Tibetan Plateau, *J. Geophys. Res.*, 117, D05102, 2012.

760 Wang, L., Sun, L.T., Shrestha, M., Li, X.P., Liu, W.B., Zhou, J., Yang, K., Lu, H., and Chen, D.L.:
761 Improving snow process modeling with satellite-based estimation of
762 near-surface-air-temperature lapse rate, *J. Geophys. Res. Atmos.*, 121, 12005-12030, 2016.

763 Xia, Y., Mitchell, K., Ek, M., Cosgrove, B., Sheffield, J., Luo, L., Alonge, C., Wei, H., Meng, J.,
764 Livneh, B., and Duang, Q.: Continental-scale water and energy flux analysis and validation for
765 North American Land Data Assimilation System project phase 2 (NLDAS-2): 2. Validation of
766 model-simulated streamflow, *J. Geophys. Res. Atmos.*, 117(D3), D03110, 2012.

- Xu, L.: The land surface water and energy budgets over the Tibetan Plateau, Available from Nature Precedings < <http://hdl.handle.net/10101/npre.2011.5587.1>>, 2011.
- Xue, B.L., Wang, L., Yang, K., Tian, L., Qin, J., Chen, Y., Zhao, L., Ma, Y., Koike, T., Hu, Z., and Li, X.P.: Modeling the land surface water and energy cycle of a mesoscale watershed in the central Tibetan Plateau with a distributed hydrological model, *J. Geophys. Res. Atmos.*, 118, 8857-8868, 2013.
- Yao, Z., Duan, R., and Liu, Z.: Changes in precipitation and air temperature and its impacts on runoff in the Nujiang River basins. *Resour. Sci.* 34(2), 202-210, 2012 (in Chinese)
- Yang, K., Qin, J., Zhao, L., Chen, Y.Y., Tang, W.J., Han, M.L., Lazhu, Chen, Z.Q., Lv, N., Ding, B.H., Wu, H., and Lin, C.G.: A multi-scale soil moisture and freeze-thaw monitoring network on the third pole, *Bull. Am. Meteorol. Soc.*, 94,1907-1916, 2013.
- Yang, K., Wu, H., Qin, J., Lin, C.G., Tang, W.J., and Chen, Y.Y.: Recent climate changes over the Tibetan Plateau and their impacts on energy and water cycle: a review, *Glob. Planet Change*, 112, 79-91, 2014.
- Yao, T.D., Thompson, L., Yang, W., Yu, W.S., Gao, Y., Guo, X.J., Yang, X.X., Duan, K.Q., Zhao, H.B., Xu, B.Q., Pu, J.C., Lu, A.X., Xiang, Y., Kattel, D.B., and Joswiak, D.: Different glacier status with atmospheric circulations in Tibetan Plateau and surroundings, *Nat. Clim. Change*, 2, 1-5, 2012.
- Yao, Y.J., Zhao, S.H., Zhang, Y.H., Jia, K., and Liu, M.: Spatial and decadal variations in potential evapotranspiration of China based on reanalysis datasets during 1982-2010, *Atmosphere*, 5, 737-754, 2014.
- Yin, G., Hu, Z.Y., Chen, X., and Tiyyip, T.: Vegetation dynamics and its response to climate change in Central Asia, *J. Arid Land*, 8, 375, 2016.
- Yu, J., Zhang, G., Yao, T., Xie, H., Zhang, H., Ke, C., and Yao, R.: Developing daily cloud-free snow composite products from MODIS Terra-Aqua and IMS for the Tibetan Plateau, *IEEE Trans. Geosci. Remote Sens.*, 54(4), 2171-2180, 2015.
- Yue, S., Pilon, P., Phinney, B., Cavadias, G.: The influence of autocorrelation on the ability to detect trend in hydrological series, *Hydrol. Process.*, 16(9), 1807-1829, 2002.
- Zhang, D., Liu, X., Zhang, Q., Liang, K., and Liu, C.: Investigation of factors affecting inter-annual variability of evapotranspiration and streamflow under different climate conditions.

797 J. Hydrol., 543, 759-769, 2016.

798 Zhang, G., Xie, H., Yao, T., Liang, T., and Kang, S.: Snow cover dynamics of four lake basins
799 over Tibetan Plateau using time series MODIS data (2001-2100), Water Resour. Res., 48(10),
800 W10529, 2012.

801 Zhang, K., Kimball, J.S., Nemani, R.R., and Running, S.W.: A continuous satellite-derived global
802 record of land surface evapotranspiration from 1983 to 2006, Water Resour. Res., 46(9),
803 W09522, 2010.

804 Zhang, L., Su, F., Yang, D., Hao, Z., and Tong, K.: Discharge regime and simulation for the
805 upstream of major rivers over Tibetan Plateau, J. Geophys. Res. Atmos., 118(15), 8500-8518,
806 2013.

807 Zhang, Q., Li, J., Singh, V., and Xu, C.: Copula-based spatial-temporal patterns of precipitation
808 extremes in China, Int. J. Climatol., 33, 1140-1152, 2013.

809 Zhang, X., Tang, Q., Pan, M., and Tang, Y.: A long-term land surface hydrologic fluxes and states
810 dataset for China, J. Hydrometeorol., 15, 2067-2084, 2014.

811 Zhang, Y., Peña-Arancibia, J.L., McVicar, T.R., Chiew, F.H.S., Vaze, J., Liu, C.M., Lu, X.J.,
812 Zheng, H.X., Wang, Y.P., Liu, Y.Y., Miralles, D.G., and Pan, M.: Multi-decadal trends in global
813 terrestrial evapotranspiration and its components, Scientific Reports, 6, 19124, 2016.

814 Zhang, Y., Liu, C., Tang, Y., and Yang, Y.: Trend in pan evaporation and reference and actual
815 evapotranspiration across the Tibetan Plateau, J. Geophys. Res., 112, D12110, 2007.

816 Zhou, C., Jia, S., Yan, H., and Yang, G.: Changing trend of water resources in Qinghai Province
817 from 1956 to 2000, J. Glaciol. Geocryol., 27(3), 432-437, 2005 (in Chinese).

818 Zhou, J., Wang, L., Zhang, Y.S., Guo, Y.H., Li, X.P., and Liu, W.B.: Exploring the water storage
819 changes in the largest lake (Selin Co) over the Tibetan Plateau during 2003-2012 from a
820 basin-wide hydrological modeling,. Water Resour. Res., 51, 8060-8086, 2015.

821 Zhou, S.Q., Kang, S., Chen, F., and Joswiak, D.R.: Water balance observations reveal significant
822 subsurface water seepage from Lake Nam Co., south-central Tibetan Plateau,. J. Hydrol., 491,
823 89-99, 2013.

824 Zhu, Y., Chen, J., Chen, G.: Runoff variation and its impacting factors in the headwaters of the
825 Yangtze River in recent 32 years, J. Yangtze River Sci. Res. Inst., 28(6), 1-4, 2011 (in Chinese).

826 **Table 1:** Overview of multi-source datasets applied in this study

Data category	Data source	Spatial resolution	Temporal resolution	Available period used	Reference
Runoff (Q)	Observed, National Hydrology Almanac of China	—	Daily	1982-2011	—
	VIC_IGSNRR simulated	0.25°	Daily	1982-2011	Zhang et al. (2014)
Precipitation (P)	Observed, CMA	0.5°	Monthly	1982-2011	—
	TRMM 3B43 V7	0.25°	Monthly	2000-2011	Huffman et al. (2012)
	IGSNRR forcing	0.25°	Daily	1982-2011	Zhang et al. (2014)
Temperature (Temp.)	Observed, CMA	0.5°	Monthly	2000-2011	—
Terrestrial storage change (ΔS)	GRACE-CSR	Approx.300-400 km	Monthly	2002-2011	Tapley et al. (2004)
	GRACE-GFZ	Approx.300-400 km	Monthly	2002-2011	Tapley et al. (2004)
	GRACE-JPL	Approx.300-400 km	Monthly	2002-2011	Tapley et al. (2004)
Potential evaporation (PET)	CRU	0.5°	Monthly	1982-2011	Harris et al. (2013)
Actual evaporation (ET)	MTE_E	0.5°	Monthly	1982-2011	Jung et al. (2010)
	VIC_E	0.25°	Daily	1982-2011	Zhang et al. (2014)
	GLEAM_E	0.25°	Daily	1982-2011	Miralles et al. (2011)
	PML_E	0.5°	Monthly	1982-2011	Zhang Y et al. (2016)
	Zhang_E	8 km	Monthly	1983-2006	Zhang et al. (2010)
	GNoah_E	1.0°	3 hourly	1982-2011	Rui (2011)
NDVI	GIMMS NDVI dataset	8 km	15 daily	1982-2011	Tucker et al. (2005)
LAI	GLASS LAI Product	0.05°	8 daily	1982-2011	Liang and Xiao (2012)
Snow Cover	TP Snow composite Products	500 m	Daily	2005-2013	Zhang et al. (2012)
SWE	VIC_IGSNRR simulated	0.25°	Daily	1982-2011	Zhang et al. (2014)
	GlobSnow-2 Product	25 km	Daily	1982-2011	Takala et al. (2011)
Glacier Area	the Second Glacier Inventory Dataset of China	—	—	2005	Guo et al. (2014)

Table 2: Main features of the 18 TP river basins used in this study. The precipitation and temperature statistics for each basin were calculated from the observed CMA datasets while the NDVI and LAI statistics were extracted from the GIMMS NDVI dataset and GLASS LAI product. The GA% and SC% represented the percentages of multiyear-mean glacier cover and snow cover in each basin which were calculated from the Second Glacier Inventory Dataset of China and the daily TP snow cover dataset (2005-2013)

No.	Station	Altitude (m)	River name	Drainage area (km ²)	Multiyear-mean (1982-2011) and basin-averaged parameters						
					Q (mm/yr)	Prec. (mm/yr)	Temp.(°C/yr)	NDVI	LAI	GA%	SC%
01	Kulukelangan	2000	Yerqiang	32880.00	158.60	128.34	-5.68	0.05	0.03	10.97	35.03
02	Tongguziluoke	1650	Yulongkashi	14575.00	151.56	134.04	-4.07	0.06	0.04	23.27	35.95
03	Numaitilangan	1880	Keliya	7358.00	103.18	137.14	-4.78	0.06	0.03	10.86	29.16
04	Zelingou	4282	Bayin	5544.00	41.42	340.68	-4.98	0.13	0.09	0.09	21.22
05	Gadatan	3823	Yellow	7893.00	200.95	566.01	-4.60	0.34	0.54	0.13	14.94
06	Xining	3225	Yellow	9022.00	99.90	503.74	0.97	0.36	0.70	0.00	10.06
07	Tongren	3697	Yellow	2832.00	149.36	533.25	-1.37	0.39	0.83	0.00	9.42
08	Tainaihai	2632	Yellow	121972.00	159.48	540.32	-2.40	0.34	0.72	0.09	15.89
09	Huangheyan	4491	Yellow	20930.00	31.18	386.42	-4.81	0.23	0.61	0.00	17.25
10	Jimai	4450	Yellow	45015.00	85.50	441.48	-4.16	0.26	0.52	0.00	20.05
11	Yajiang	2599	Yalong	67514.00	237.66	717.05	-0.23	0.43	0.80	0.15	18.36
12	Zhimenda	3540	Yangtze	137704.00	96.23	405.66	-4.83	0.20	0.26	0.96	17.87
13	Jiaoyuqiao	3000	Salween	72844.00	364.26	620.88	-1.89	0.29	0.44	2.02	23.73
14	Pangduo	5015	Brahmaputra	16459.00	348.31	544.59	-1.53	0.27	0.33	1.66	23.33
15	Tangjia	4982	Brahmaputra	20143.00	350.61	555.17	-1.89	0.27	0.34	1.39	21.83
16	Gongbujiangda	4927	Brahmaputra	6417.00	586.96	692.06	-4.24	0.27	0.36	4.12	25.99
17	Nuxia	2910	Brahmaputra	191235.00	307.38	401.35	-0.73	0.22	0.25	1.90	13.50
18	Yangcun	3600	Brahmaputra	152701.00	163.25	349.91	-0.87	0.19	0.18	1.28	10.52

833 **Table 3:** Annual-averaged water storage changes (ΔS) in 18 TP basins derived from GRACE retrievals (2002-2013) from three different processing centers (CSR,
834 GFZ and JPL)
835

Basin	Water storage Change (ΔS ,mm)		
	CSR	GFZ	JPL
Kulukelangan	-0.16	-0.16	-0.00
Tongguziluoke	0.10	0.10	0.28
Numaitilangan	0.24	0.22	0.41
Zelingou	0.63	0.41	0.69
Gadatan	0.02	-0.24	-0.03
Xining	-0.08	-0.35	-0.14
Tongren	-0.13	-0.41	-0.21
Tainaihai	0.12	-0.16	0.10
Huangheyan	0.60	0.35	0.70
Jimai	0.41	0.15	0.48
Yajiang	-0.23	-0.50	-0.21
Zhimenda	0.57	0.38	0.78
Jiaoyuqiao	-1.00	-1.13	-0.79
Nuxia	-1.42	-1.44	-1.31
Pangduo	-1.21	-1.29	-1.02
Tangjia	-1.40	-1.46	-1.24
Gongbujiangda	-1.61	-1.67	-1.47
Yangcun	-1.33	-1.34	-1.21

836
837

838 **Table 4:** Nonparametric trends for different ET estimates during the period 1982-2006 detected by modified Mann-Kendall test, the bold number showed the
839 detected trend is statistically significant at the 0.05 level

841	Basin	ET _{wb}	GLEAM_E	VIC_E	Zhang_E	PML_E	MET_E	GNoah_E
842	Kulukelangan	-0.09	0.09	0.18	—	0.03	-0.01	0.07
	Tongguziluoke	-0.02	0.10	0.13	—	0.03	-0.08	0.19
843	Numaitilangan	0.04	0.10	0.14	—	0.14	-0.10	0.22
	Zelingou	0.13	0.23	0.11	0.09	0.04	0.06	0.02
844	Gadatan	-0.09	0.25	0.070	-0.10	-0.01	0.06	-0.07
	Xining	-0.06	0.54	0.01	-0.08	0.01	0.02	-0.06
845	Tongren	-0.06	0.34	-0.15	-0.17	0.07	0.02	0.13
	Tainaihai	0.06	0.28	-0.03	-0.11	0.04	0.05	0.04
846	Huangheyan	0.08	0.19	-0.01	-0.10	0.08	0.05	0.10
	Jimai	-0.07	0.23	-0.01	-0.08	0.03	0.05	0.10
847	Yajiang	0.17	0.26	0.06	-0.21	-0.01	0.03	-0.02
	Zhimenda	0.11	0.28	0.10	0.01	0.07	0.04	0.07
848	Jiaoyuqiao	0.18	0.28	0.10	-0.11	0.05	0.05	0.07
	Nuxia	-0.09	0.25	0.09	-0.10	0.12	0.04	0.10
849	Pangduo	0.05	0.28	0.17	-0.07	0.07	0.07	0.11
	Tangjia	0.09	0.26	0.17	-0.09	0.20	0.06	0.12
850	Gongbujiangda	-0.26	0.12	0.13	-0.16	0.19	0.01	0.15
	Yangcun	0.03	0.28	0.08	-0.06	0.10	0.04	0.09

Figure captions:

Figure1. Map of river basins and hydrological gauging stations (green dots) over the Tibetan Plateau (TP) used in this study. The grey shading shows the topography of TP in meters above the sea level and the blue shading exhibits the glaciers distribution in TP extracted from the Second Glacier Inventory Dataset of China.

Figure 2. Comparison of VIC_IGSNRR simulated and observed monthly runoff for Tangnaihai and Panduo stations (a and b) as well as (c) basin-averaged monthly TRMM, CMA gridded and IGSNRR forcing precipitations for the smallest basin (Tongren station) over the period 1982-2011. (d) shows the comparison of TRMM (blue) and IGSNRR forcing (red) precipitations against CMA gridded precipitation for 18 river basins over TP during the period 2000-2011.

Figure 3. Comparison of different ET products against the calculated ET through the water balance method (ET_{wb}) at the monthly time scale for 18 TP basins during the period 1983-2006. The boxplot of monthly estimates of different ET products for 18 TP basins are shown in (a) while the correlation coefficients and root-mean-square-errors (RMSEs, mm/month) for each ET product relatively to ET_{wb} are exhibited in (b).

Figure 4. General water and energy status (a. the perspective of Budyko framework) and their relationships with glacier (b) and vegetation (c and d) for eighteen TP river basins (1983-2006). The ET used in this figure is calculated from the bias-corrected water balance method.

Figure 5. Seasonal cycles (1982-2011) of water budget components in westerlies-dominated (column 1), East Asian monsoon-dominated (columns 2-4) and Indian monsoon-dominated (columns 5-6) TP basins.

Figure 6. Seasonal cycles (1982-2011) of air temperature and vegetation parameters in westerlies-dominated (column 1), East Asian monsoon-dominated (columns 2-4) and Indian monsoon-dominated (columns 5-6) TP basins.

Figure 7. Seasonal cycles (1982-2011) of snow cover and snow water equivalent (SWE) in westerlies-dominated (column 1), East Asian monsoon-dominated (columns

2-4) and Indian monsoon-dominated (columns 5-6) TP basins. The snow cover was extracted from cloud free snow composite product during the period 2005-2013. It should also be noted that the GlobSnow data are not available for some basins.

Figure 8. Sen's slopes of water budget components and vegetation parameters in westerlies-dominated TP basins during the period of 1982-2011. To clearly exhibit the nonparametric trends of all variables in one panel, the Sen's Slopes of Q, P, ET_{wb} and PET have been multiplied by 1/12 (unit: mm/month). The double red stars showed that the trend was statistically significant at the 0.05 level.

Figure 9. Linear and non-parametric trends of westerly, Indian monsoon and East Asian summer monsoon during the period 1982-2011 revealed prospectively by the Asian Zonal Circulation Index, Indian Ocean Dipole Mode Index and East Asian Summer Monsoon Index.

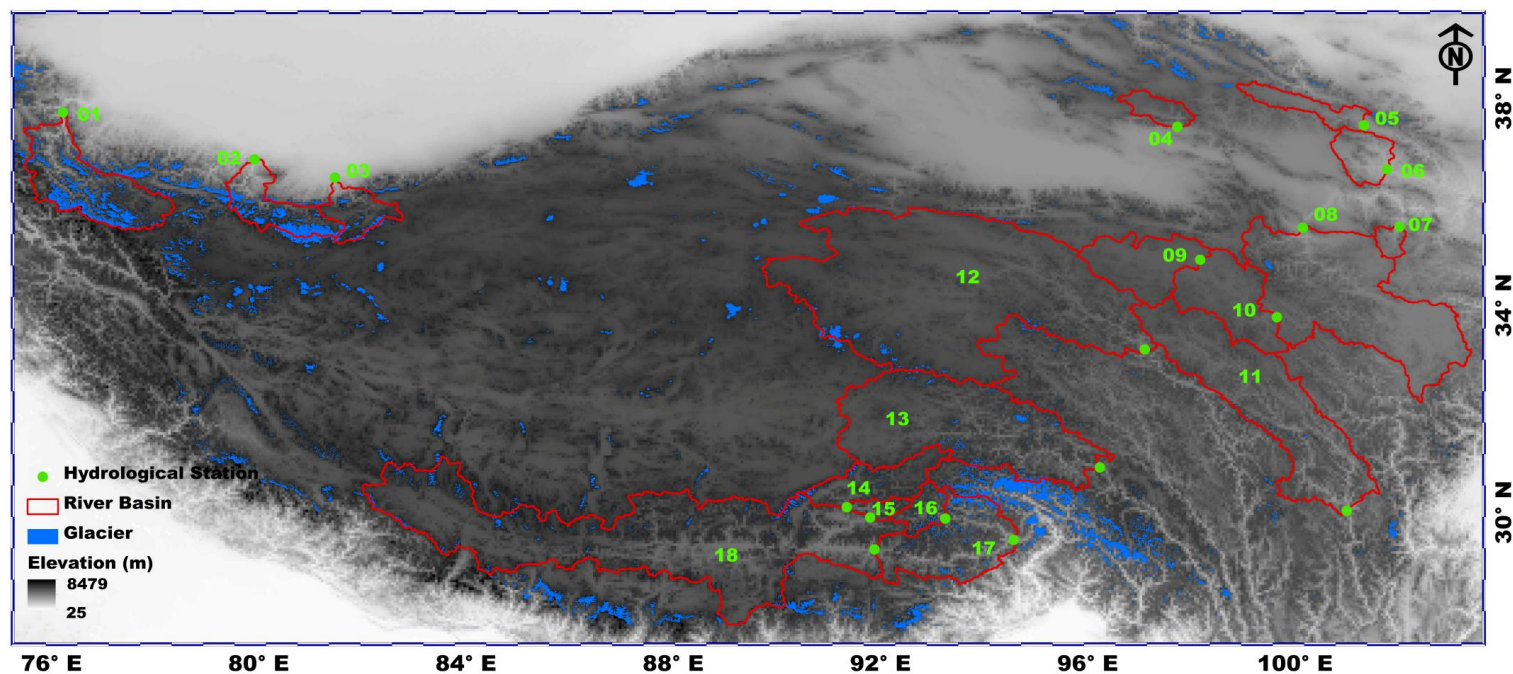
Figure 10. Similar to Figure 8 but for East Asian monsoon-dominated TP basins. It should be noted that the GlobSnow data are not available for some basins. The double red stars showed that the trend was statistically significant at the 0.05 level.

Figure 11. Similar to Figure 8 but for Indian monsoon-dominated TP basins. It should be noted that the GlobSnow data are not available for some basins. The double red stars showed that the trend was statistically significant at the 0.05 level.

Figure 12. Uncertainties in seasonal cycles of ET_{wb} calculated from three precipitation products (CMA gridded, IGSNRR_Forcing and TRMM precipitation) in 18 TP basins. The comparisons were conducted during the period 2000-2011 when TRMM data was available.

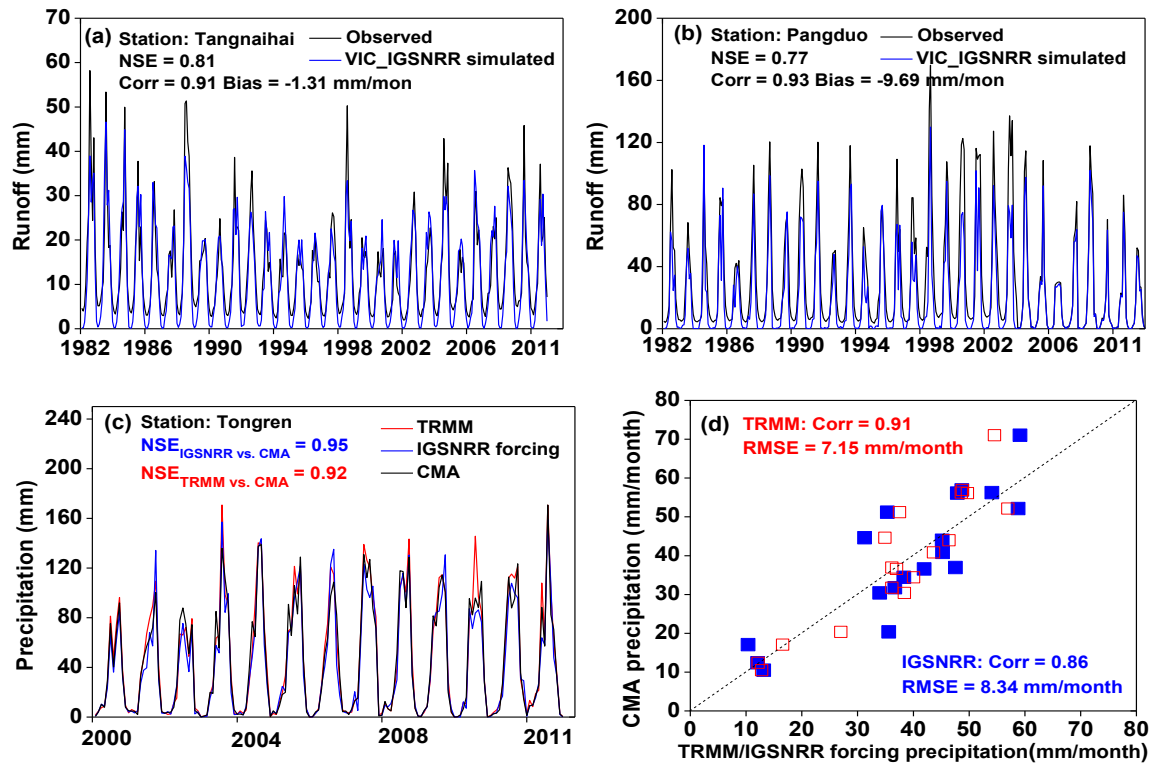
Figure 13. Uncertainties in annual trends of ET_{wb} (b) calculated from two precipitation products (CMA gridded and IGSNRR_Forcing) (a) in 18 TP basins. The comparisons were conducted during the period 1982-2011 (TRMM data was not available for the whole period).

908 **Figure 1.** Map of river basins and hydrological gauging stations (green dots) over the Tibetan Plateau (TP) used in this study. The grey shading shows the
909 topography of TP in meters above the sea level and the blue shading exhibits the glaciers distribution in TP extracted from the Second Glacier Inventory Dataset of
910 China.

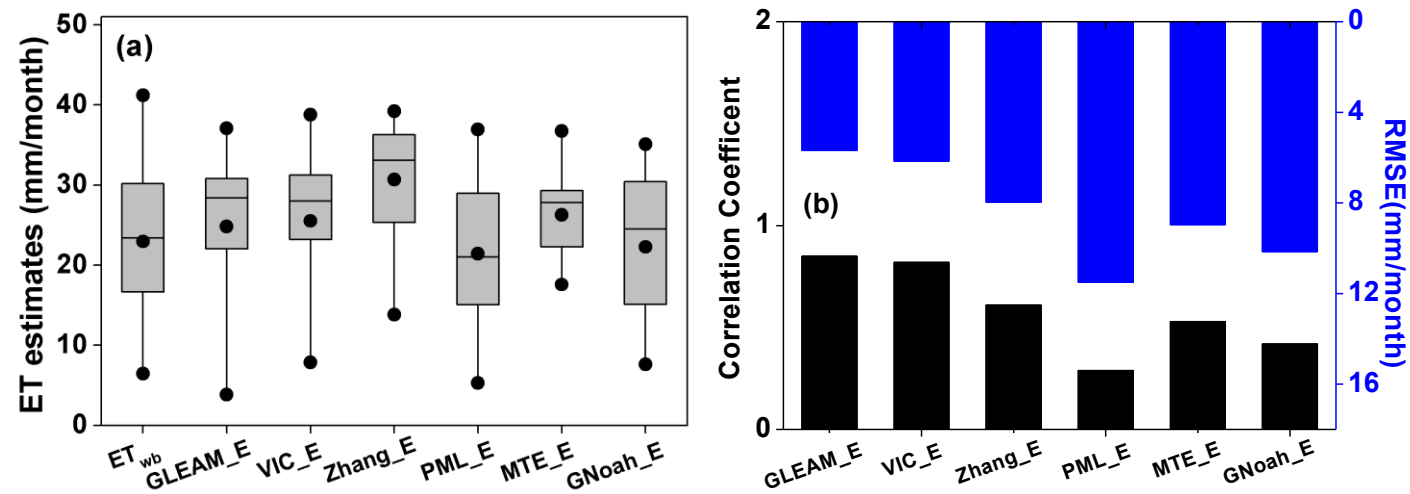


911
912

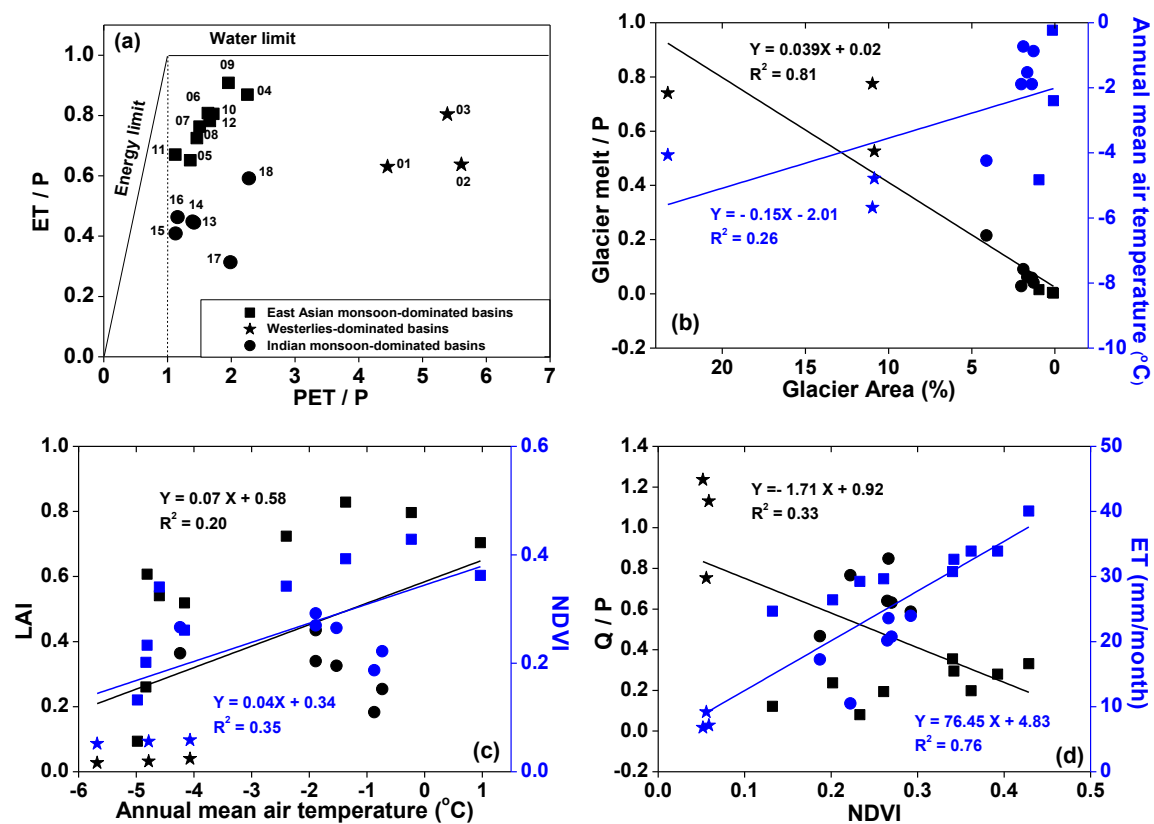
913 **Figure 2.** Comparison of VIC_IGSNRR simulated and observed monthly runoff for Tangnaihai and Panduo stations (a and b) as well as (c) basin-averaged
 914 monthly TRMM, CMA gridded and IGSNRR forcing precipitations for the smallest basin (Tongren station) over the period 1982-2011. (d) shows the comparison of
 915 TRMM (blue) and IGSNRR forcing (red) precipitations against CMA gridded precipitation for 18 river basins over TP during the period 2000-2011.



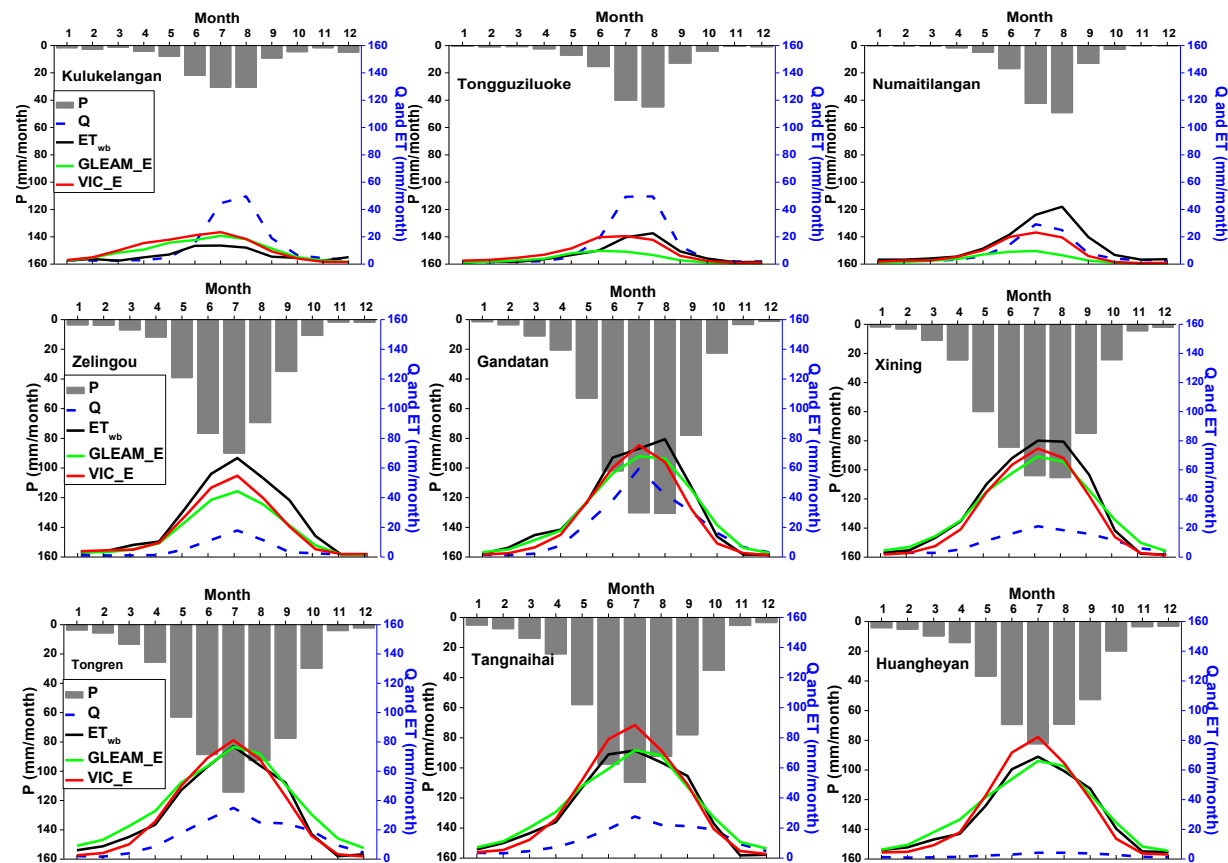
919 **Figure 3.** Comparison of different ET products against the calculated ET through the water balance (ET_{wb}) at the monthly time scale for 18 river basins over the
920 Tibetan Plateau during the period 1983-2006. The boxplot of monthly estimates of different ET products for 18 TP basins are shown in (a) while the correlation
921 coefficients and root-mean-square-errors (RMSEs, mm/month) for each ET product relatively to ET_{wb} are exhibited in (b).



924 **Figure 4.** General water and energy status (a. the perspective of Budyko framework) and their relationships with glacier (b) and vegetation (c and d) for eighteen
925 TP river basins (1983-2006). The ET used in this figure is calculated from the bias-corrected water balance method.



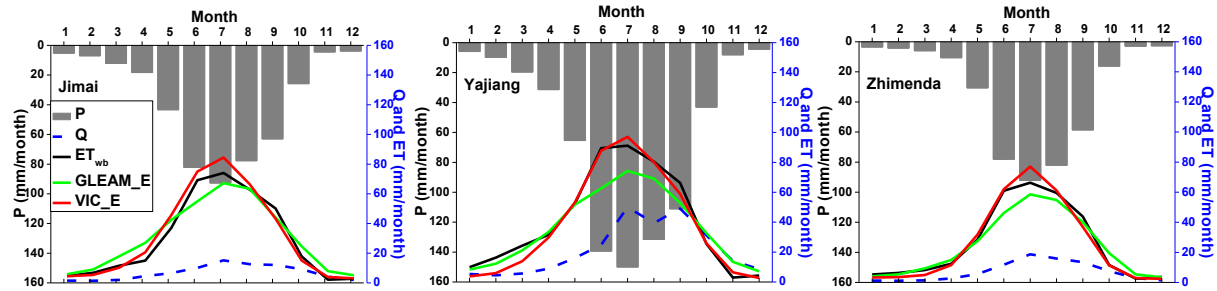
928 **Figure 5.** Seasonal cycles (1982-2011) of water budget components in westerlies-dominated (column 1), East Asian monsoon-dominated (columns 2-4) and Indian
 929 monsoon-dominated (columns 5-6) TP basins.



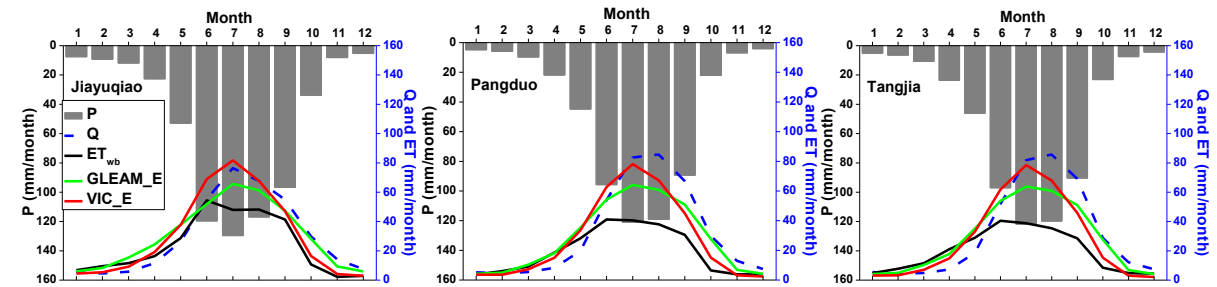
933

Figure 5: (continued)

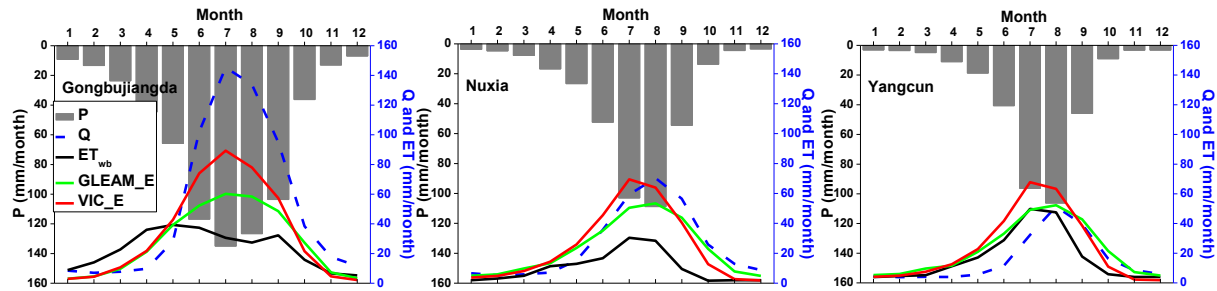
934



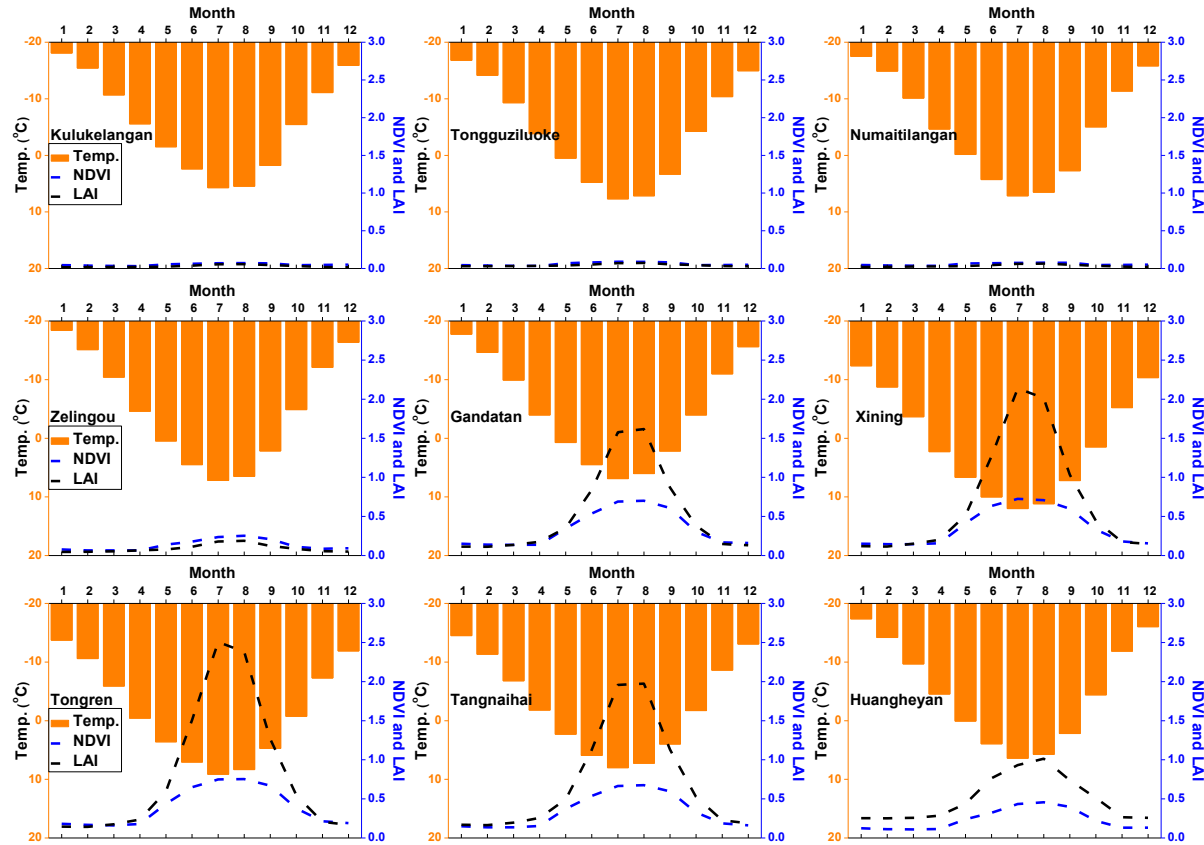
935



936



937 **Figure 6.** Seasonal cycles (1982-2011) of air temperature and vegetation parameters in westerlies-dominated (column 1), East Asian monsoon-dominated (columns
938 2-4) and Indian monsoon-dominated (columns 5-6) TP basins.



942

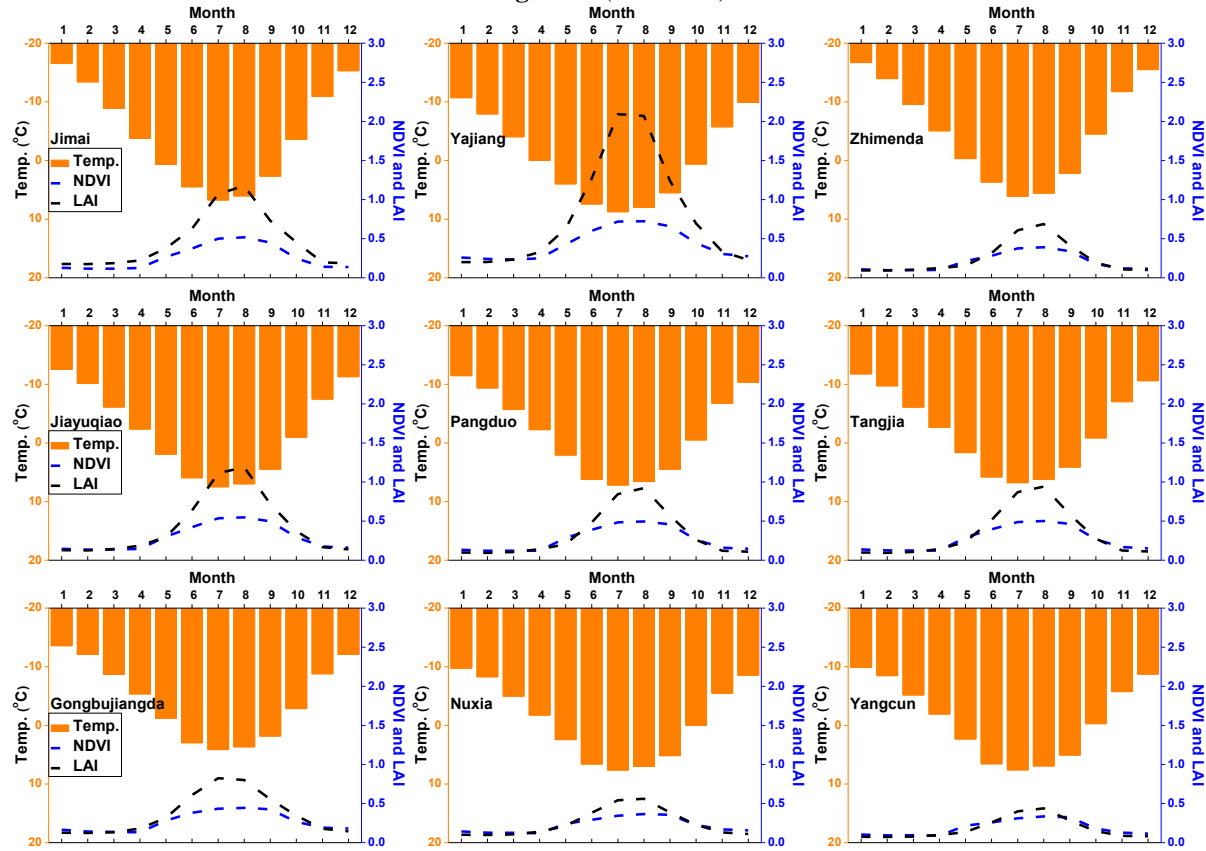
943

944

945

946

Figure 6: (continued)



947 **Figure 7.** Seasonal cycles (1982-2011) of snow cover and snow water equivalent (SWE) in westerlies-dominated (column 1), East Asian monsoon- dominated
948 (columns 2-4) and Indian monsoon-dominated (columns 5-6) TP basins. The snow cover was extracted from cloud free snow composite product during the period
949 2005-2013. It should also be noted that the GlobSnow data are not available for some basins.
950

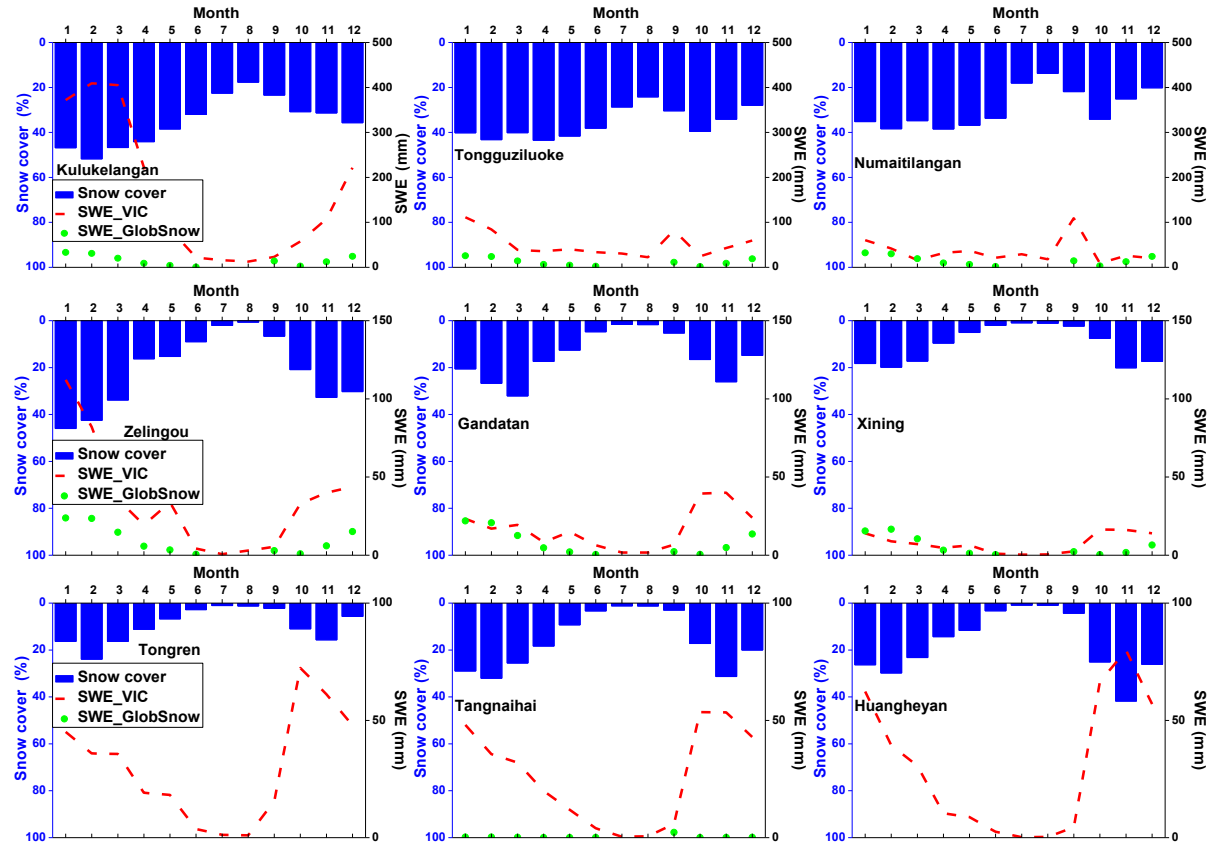
951

952

953

954

955



956

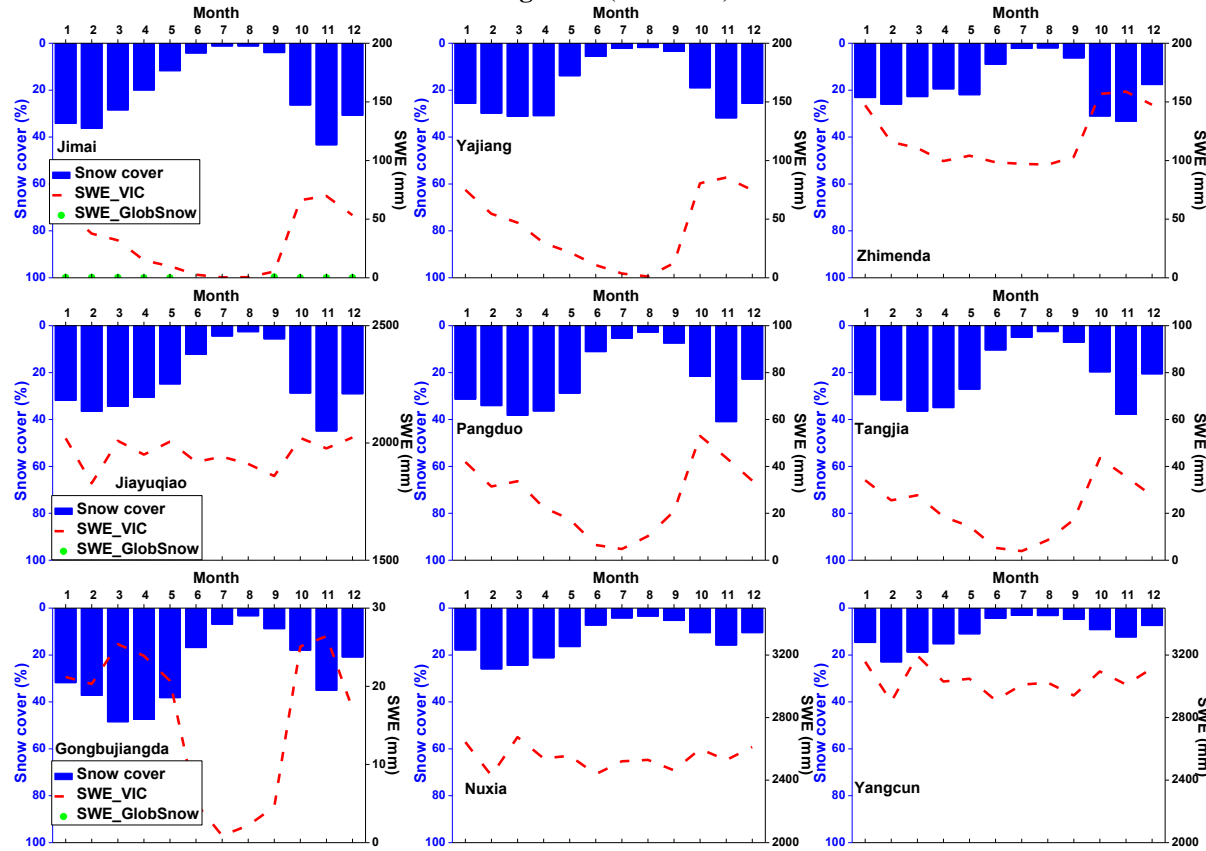
957

958

959

960

Figure 7: (continued)



961 **Figure 8.** Sen's slopes of water budget components and vegetation parameters in westerlies-dominated TP basins during the period of 1982-2011. To clearly
962 exhibit the nonparametric trends of all variables in one panel, the Sen's Slopes of Q, P, ET_{wb} and PET have been multiplied by 1/12 (unit: mm/month). The double
963 red stars showed that the trend was statistically significant at the 0.05 level.

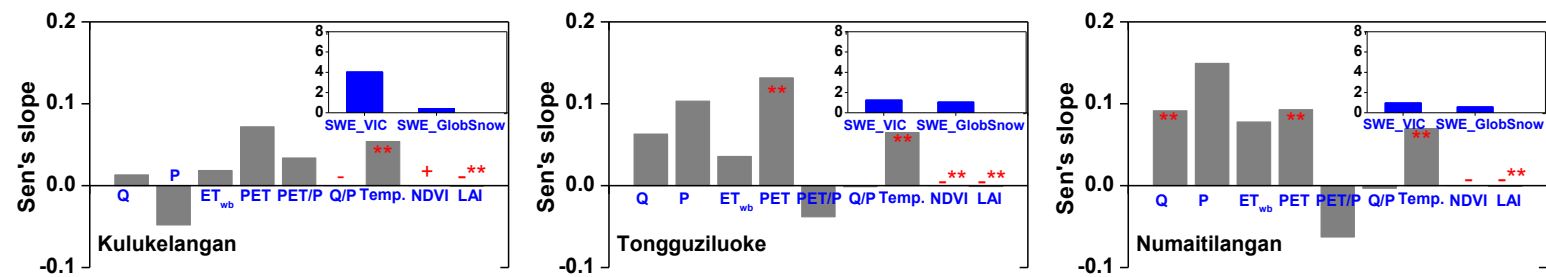
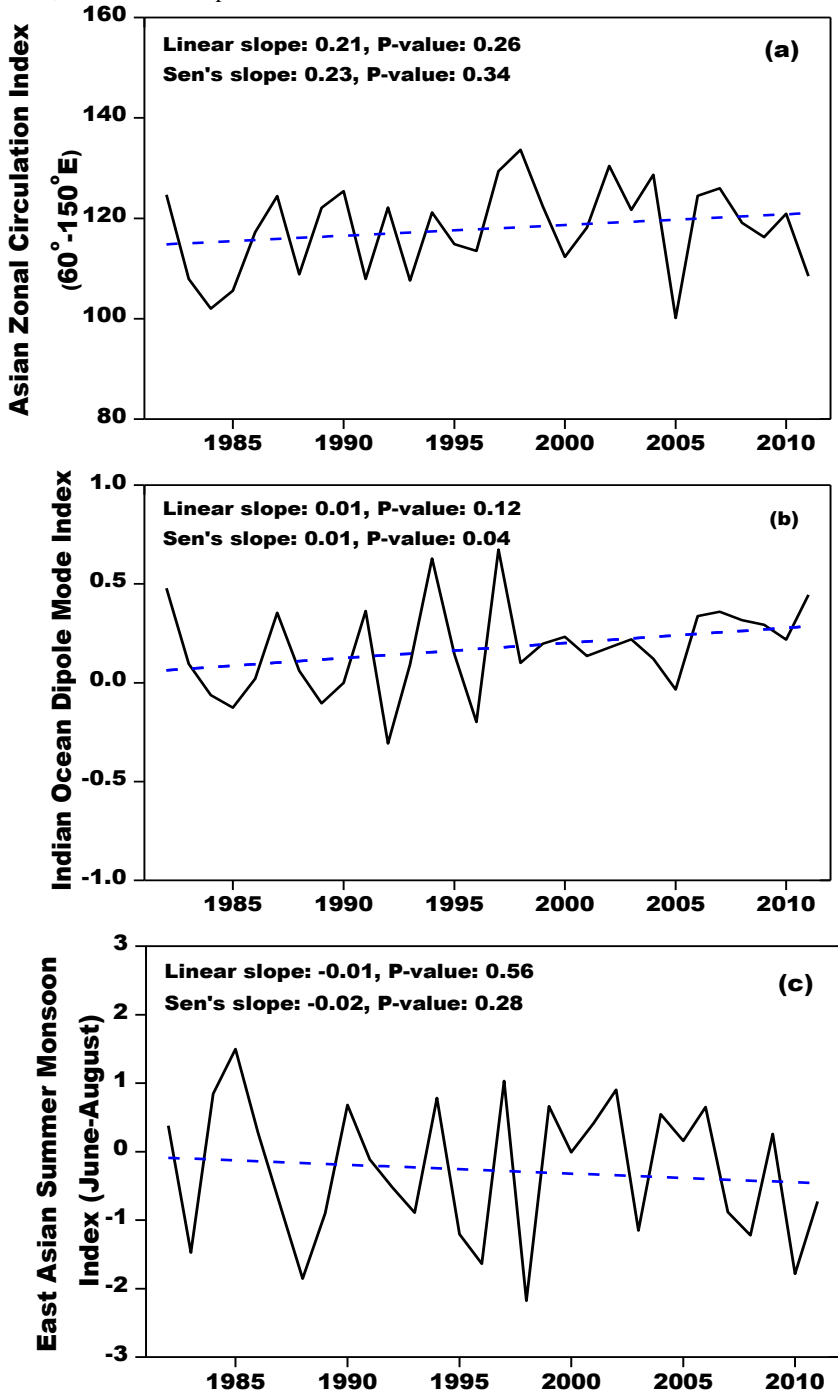
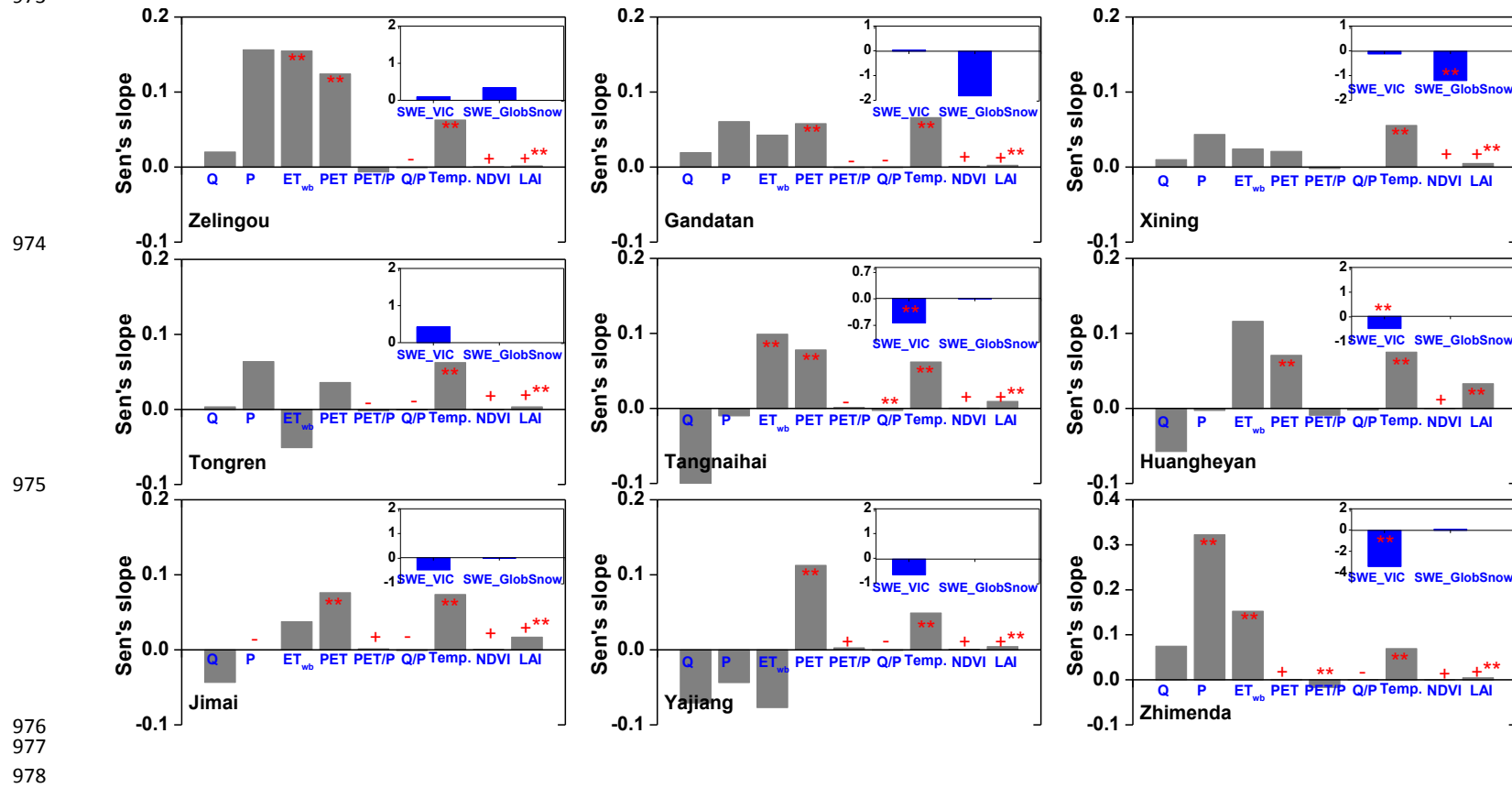


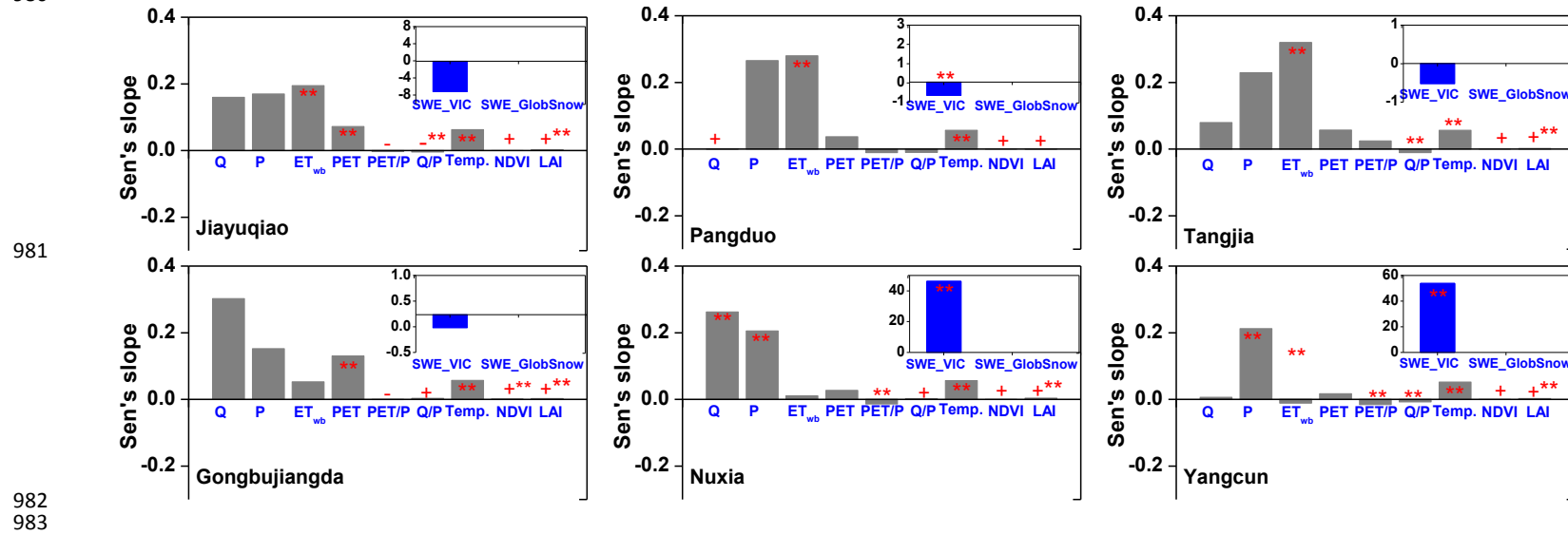
Figure 9. Linear and non-parametric trends of westerly, Indian monsoon and East Asian summer monsoon during the period 1982-2011 revealed prospectively by the Asian Zonal Circulation Index, Indian Ocean Dipole Mode Index and East Asian Summer Monsoon Index.



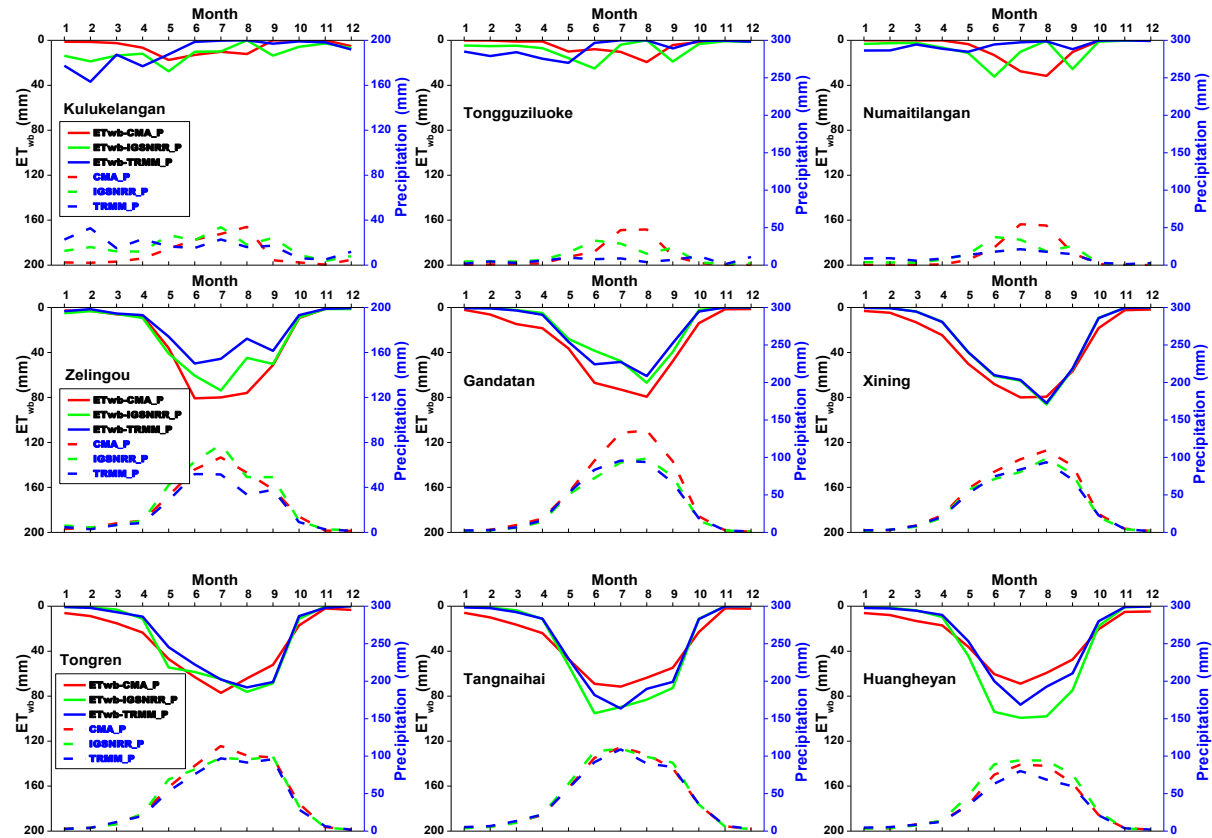
972 **Figure 10.** Similar to Figure 8 but for East Asian monsoon-dominated TP basins. It should be noted that the GlobSnow data are not available for some basins.
 973



979 **Figure 11.** Similar to Figure 8 but for Indian monsoon-dominated TP basins. It should be noted that the GlobSnow data are not available for some basins.
 980



984 **Figure 12.** Uncertainties in seasonal cycles of ET_{wb} calculated from three precipitation products (CMA gridded, IGSNRR_Forcings and TRMM precipitation) in 18 TP
 985 basins. The comparisons were conducted during the period 2000-2011 when TRMM data was available.



990

991

992

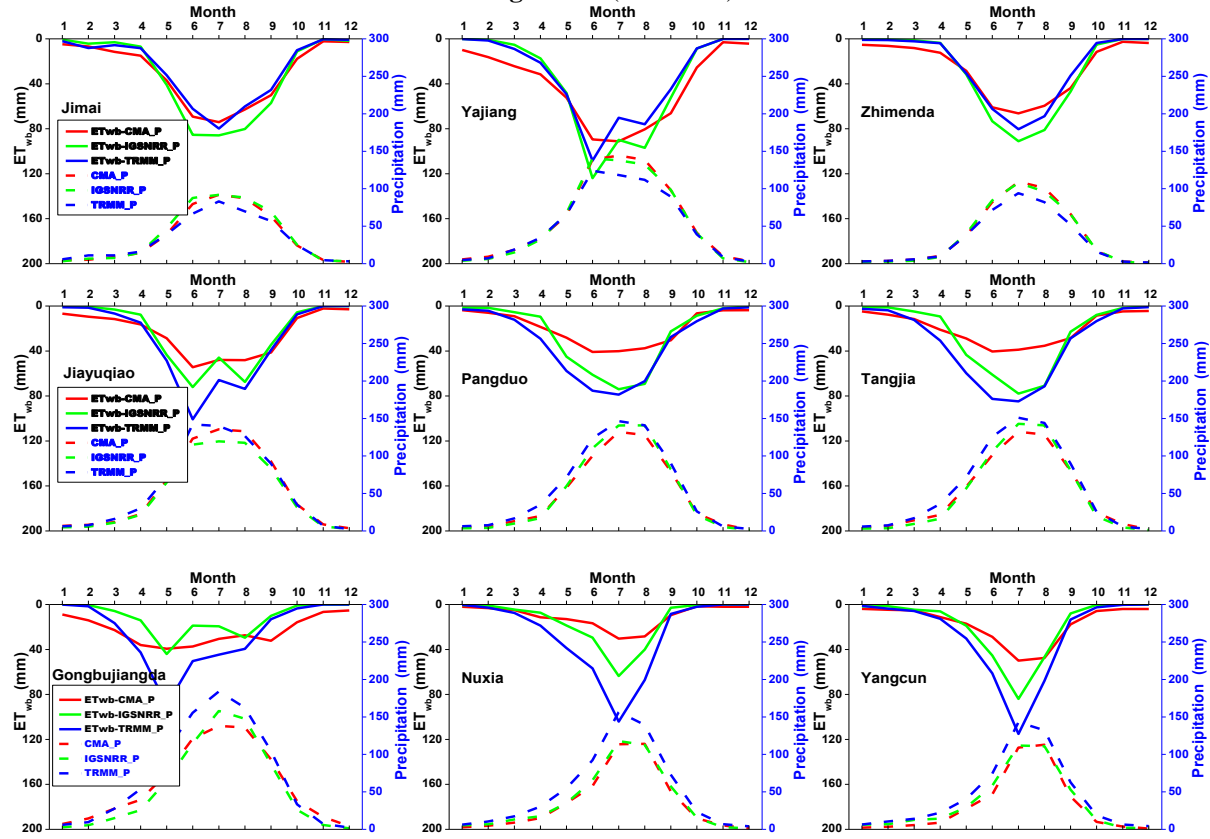
993

994

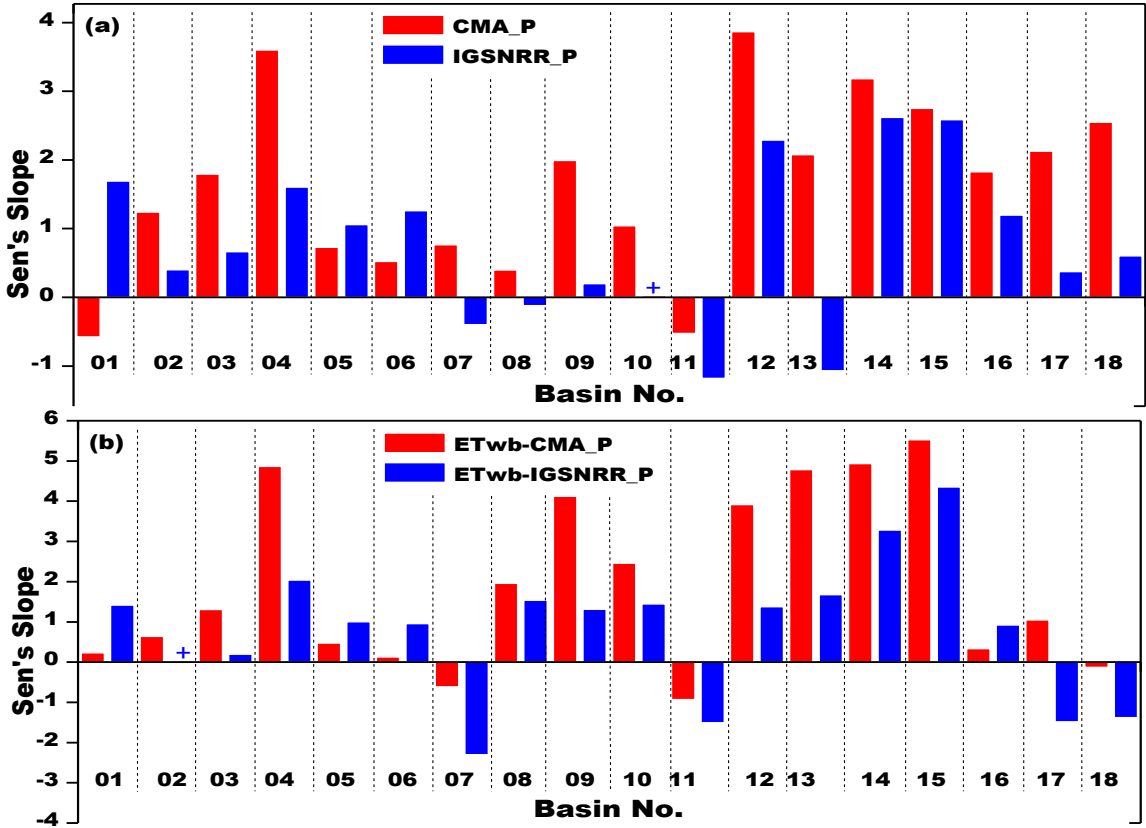
995

996

Figure 12: (continued)



997 **Figure 13.** Uncertainties in annual trends of ET_{wb} (b) calculated from two precipitation products (CMA gridded and IGSNRR_Forcings) (a) in 18 TP basins. The
 998 comparisons were conducted during the period 1982-2011 (TRMM data was not available for the whole period).



999

1000